

https://dspace.org/

The effect of thermal shock on the abrasive wear of WC-12wt%Co

Makgere, Machoene Frederick

2009-03-25T10:08:31Z
http://hdl.handle.net/10539/6798

Downloaded from a DSpace repository. https://dspace.org/

4. RESULTS AND DISCUSSION

4.1 Sample characterization

Sample characterization before the tests was done to detect any manufacturing flaws and factors that may influence the tests. This section presents results on the WC grain size, Co mean free path, hardness and density of the WC-12wt%Co samples. The results will be compared to those given by the supplier BOART LONGYEAR to compare the quality measurements (see Table 4.1). Some of these properties are known to affect the abrasive wear. Below is a typical micrograph of the WC-12wt%Co alloy used for this project.

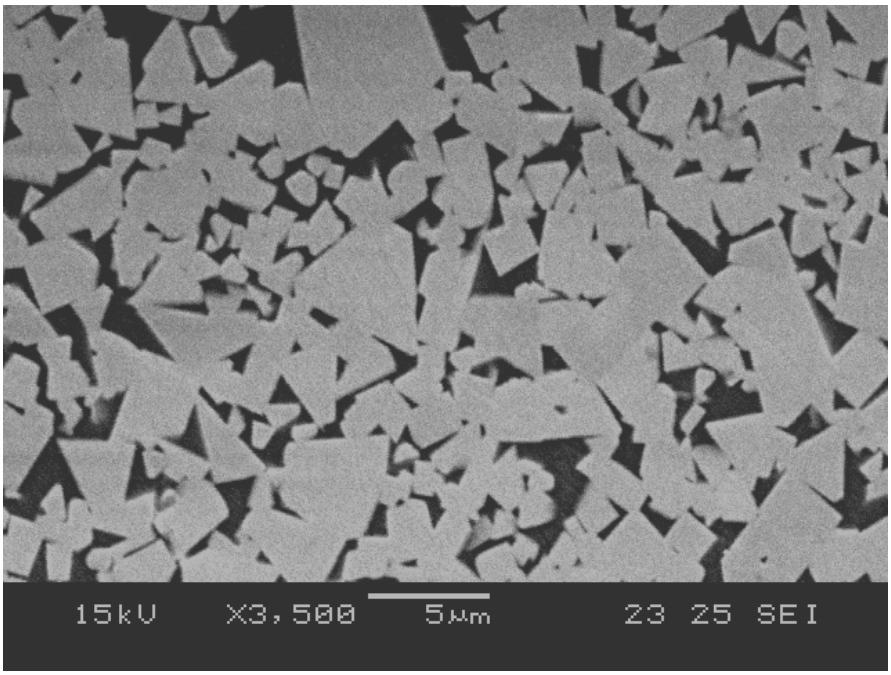


Figure 4.1: Microstructure of WC-12wt%Co. The grey angular particles are hard WC grains and the dark material between the WC grains is Co.

Table 4.1: Nominal properties of WC-12wt%Co from BOART LONGYEAR.

Hardness (HV)	1200
WC grain size ((μm)	1.9
Density (g/cm^3)	14.33
Thermal expansion coefficient ($10^{-6}/K$)	6.4
Abrasion Resistance (cm^{-3})	1.2
Fracture toughness (MPa $m^{1/2}$)	15.6

4.1.1 Vickers hardness

WC-Co alloys are known to be hard and brittle. The average of 10 measurements using an indentation load of 30Kgf was used to determine the hardness of the WC-12wt%Co. The mean value obtained was 1160 ± 13.5 HV which is close to the value listed in table 4.1.

4.1.2 WC grain size and Co mean free path

The mean WC grain size and the Co mean free path are given in table 4.2 and illustrated graphically in Figures 4.2 and 4.3. The medians were determined from Figures 4.2 and 4.3 to obtain the WC grain size and the cobalt mean free path while the averages indicates the mean values. The average WC grain size given by BOART LONGYEAR is 1.9μm, which is close to the measured mean value in Table 4.2.

Table 4.2: Mean WC grain size and Co mean free path of WC-12wt%Co.

	WC grain size (μm)	Mean free path (μm)
Median	1.55±1.04	0.40±0.039
Average	2.03±1.04	0.53±0.039

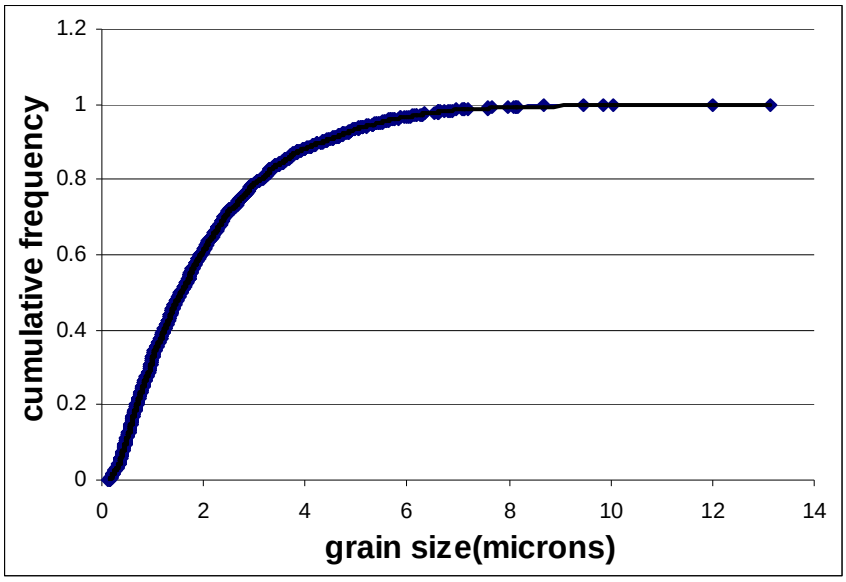


Figure 4.2: WC grain size distribution of the WC-12wt%Co alloy.

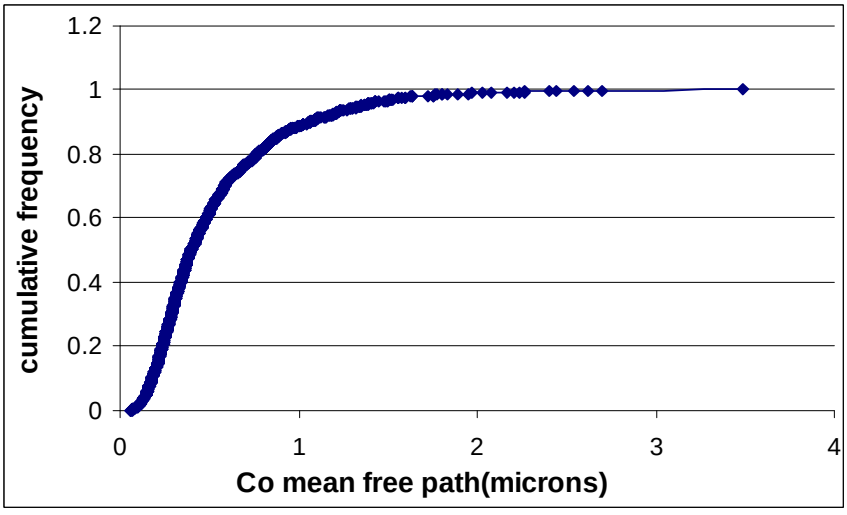


Figure 4.3: Mean free path distribution of the WC-12wt%Co alloy.

4.1.3 Density

The density was measured using the Archimedes principle as described in section 3.2.3. Table 4.3 shows the density measurements of WC-12wt%Co taken from three samples. The average density value measured is 14.15g/cm^3 which is close to the value given in table 4.1.

Table 4.3: Density measurements of WC-12wt%Co alloy.

	Wt_{air} (g)	Wt_{water} (g)	Density (g/cm^3)
Sample 1	4.90	4.58	14.31
Sample 2	3.47	3.24	14.10
Sample 3	4.96	4.63	14.03
Average			14.15 ± 0.16

4.2 Abrasive wear response

Abrasive wear tests were performed on 80-grit SiC abrasive paper using a 2-body sliding wear apparatus on samples before and after thermal shock as described in section 3.4.

4.2.1 Effect of thermal shock temperature on abrasive wear

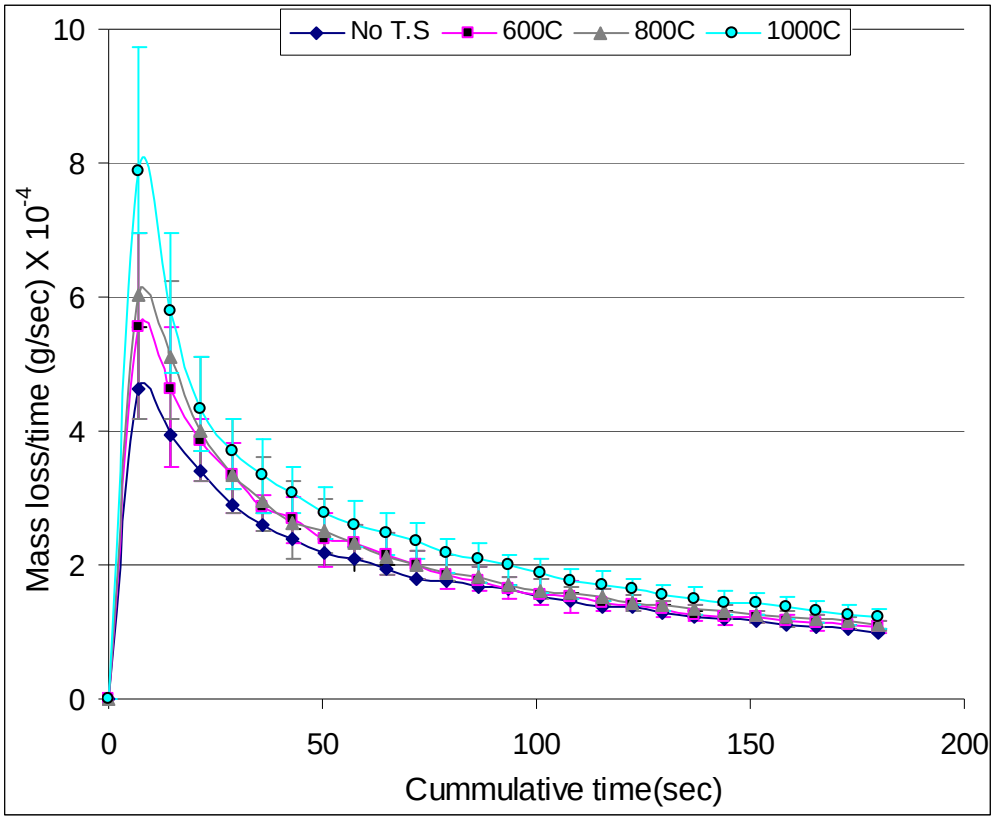


Figure 4.4: Effect of thermal shock temperature at constant 60 thermal shock cycles on the mass loss rate of WC-12wt%Co.

The data shows an initial high mass loss rate during the first 40 seconds, which increases with increasing temperature, see Figure 4.4. Initially the abrasive particles are sharp and angular and so the stress is high, hence the initial high wear rate for all the tests. With regard to increases with increasing temperature, the surface layer may have been damaged by depletion of cobalt, cracks or oxidation on and below the surface which results in this high wear rate at the beginning. SEM analysis, which is described in Section 4.3, verified the random cobalt depletion.

Eventually the rate of mass loss converges for all the samples. This implies that the specimens have only been damaged down to a certain surface depth and once the damaged layer has been removed during abrasion, all specimens wear at the same rate. The damaged surface depth differs because the convergence of the wear rates is not simultaneous. This implies that from a certain depth, the samples subjected to thermal shock behave in the same way as the samples without thermal shock. The time required for the convergence increases with increasing thermal shock temperature suggesting that the damaged layer increases in depth with temperature.

The increase in wear rate at the beginning of the test is higher when going from 800°C to 1000°C than from 600°C to 800°C. These suggest that the severest damage occurred at 1000°C. Previous studies by Xiao Han [38] showed that the cobalt becomes lava-like at 1000°C and retains this structure down to room temperature. This may result in high losses during abrasive wear. Consequently higher cumulative mass losses were observed for samples subjected to thermal shock at that temperature, see Figure 4.5.

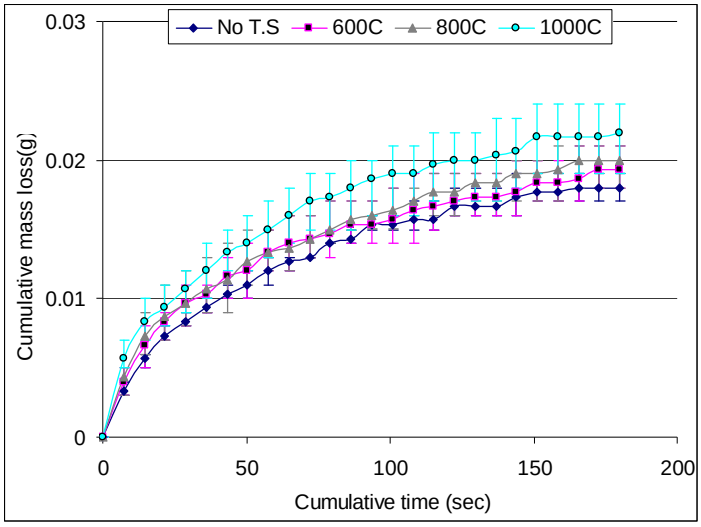


Figure 4.5: Effect of thermal shock temperature at constant 60 thermal shock cycles on the mass loss of WC-12wt%Co.

This initial high mass loss response is magnified possibly hundreds of times when drill bits are subjected to severe thermal shock and wear simultaneously in industry and for many more cycles than those tested here. The data of the mass loss per time graphs are given in Appendix B.

4.2.2 Effect of thermal shock cycles on abrasive wear

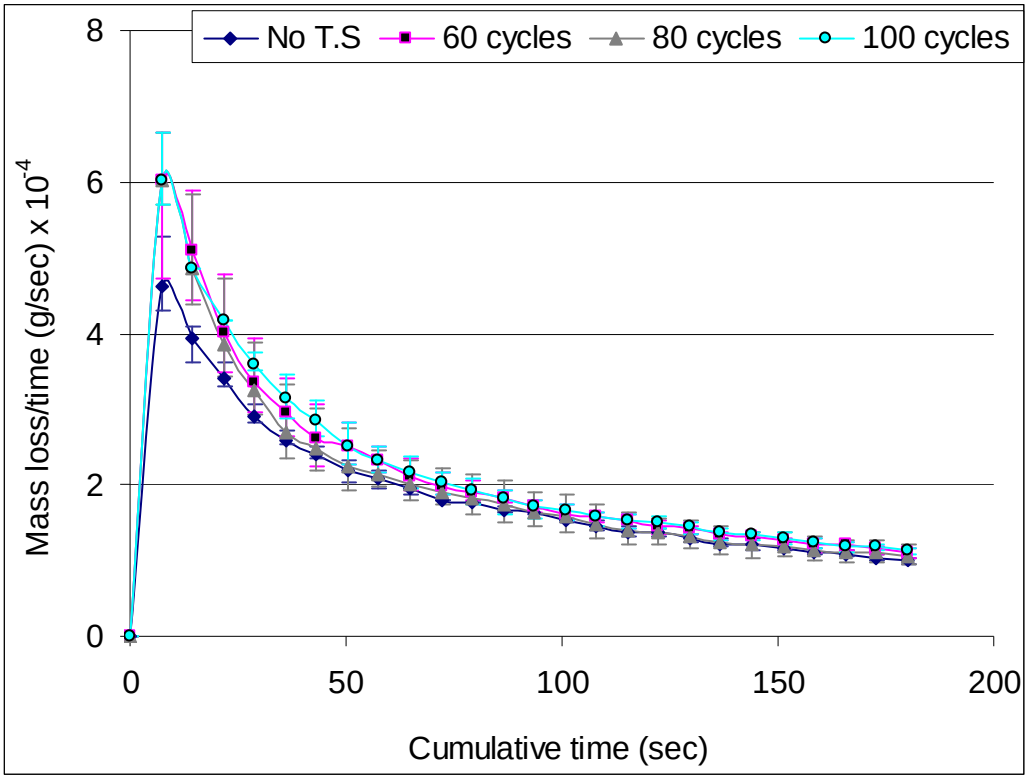


Figure 4.6: Effect of thermal shock cycles at constant thermal shock temperature of 800°C on the mass loss rate of WC-12wt%Co.

An initial high mass loss is observed when the samples are subjected to thermal shock cycles at constant temperature (see Figure 4.6). However there is no significant mass loss difference with respect to thermal shock cycles. This may suggest that the difference in thermal shock cycles was not large enough to cause a difference in wear

rate. Figure 4.7 shows a graph of cumulative mass loss versus cumulative time where again there is no significant difference when varying thermal shock cycles. Next sections will try to explain effects of these behaviours by analyzing the samples after thermal shock.

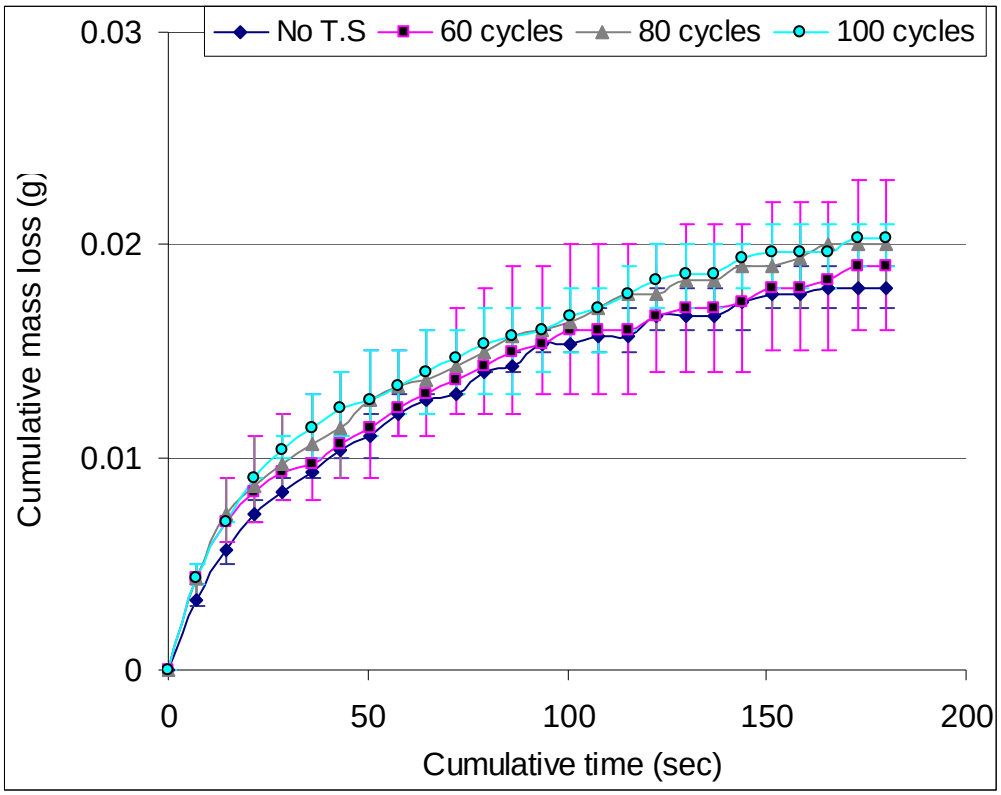


Figure 4.7: Effect of thermal shock cycles at constant thermal shock temperature of 800°C on the cumulative mass loss of WC-12wt%Co.

4.2.3 Abraded surface layer analysis

Using the density of the material, 14.15 g/cm^3 (obtained in this project) and assuming that the density of the surface remains the same after thermal shock (although it certainly does not), the volume loss was measured after ~7 seconds of abrasive wear,

i.e. when the wear rate was highest. Then, the thickness of the layer removed in ~7 sec was calculated by dividing the volume loss by the area in contact with the SiC abrasive. This was done because the initial high mass loss that was observed after ~7 seconds will be repeated over and over during drilling where thermal shock and abrasive wear occur at the same time. These analyses were done on the area that was previously polished. The test area of the specimen was "Lx b ~ 30cm^2" which is the phase that was originally polished; refer to Figure 4.9. Although in industry the material is subjected to more severe conditions than those applied here i.e. longer drilling times. Table 4.4 and Figure 4.8 report the results of these calculations.

Table 4.4: Mass loss and the thickness of layer removed during the initial ~7 seconds of abrasion, assuming the density of the lost mass to be 14.33g/cm^3 and 14.15g/cm^3

	Mass loss after 7 seconds (g)	Thickness layer removed (µm) density=14.33g/cm^3	Thickness layer removed (µm) Density=14.15g/cm^3
No T.S (20°C)	0.0033 ± 0.00058	7.68	7.85
600°C (60 cycles)	0.0040 ± 0.001	9.30	9.42
800°C (60 cycles)	0.0043 ± 0.0012	10.00	10.13
800°C (80 cycles)	0.0043 ± 0.00058	10.00	10.13
800°C (100 cycles)	0.0043 ± 0.00058	10.00	10.13
1000°C (60 cycles)	0.0057 ± 0.0012	13.26	13.43

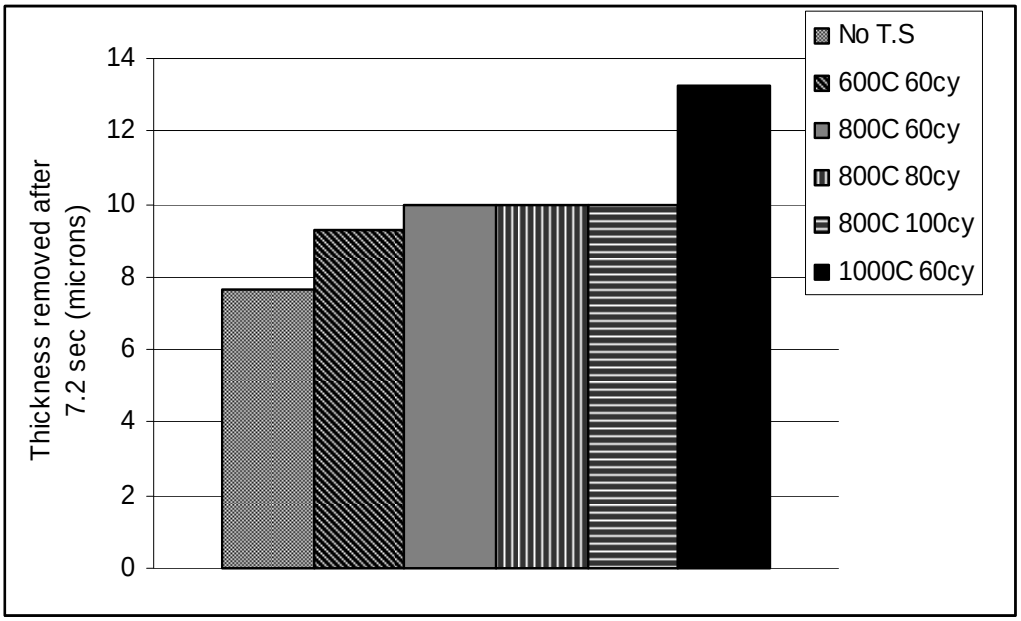


Figure 4.8: Effect of temperature and number of thermal shock cycles at the thickness of the layer removed after the initial ~7 seconds of abrasion.

Table 4.4 and Figure 4.8 show that at 1000°C the thickest layer was removed after ~7 sec.

The thickness of the layer removed after 180 seconds i.e. at the end of the test was also measured (see Table 4.5). From Table 4.5 it is clear that as temperature increases so does the thickness of the removed layer.

Table 4.5: Mass loss and thickness of removed layer after 180 sec.

	Mass loss after 180 sec (g)	Removed layer thickness (µm)	Differences in removed layer thickness (µm)
No T.S (20°C)	0.018 ± 0.001	41.87	0
600°C (60 cycles)	0.019 ± 0.0015	44.97	3.1
800°C (60 cycles)	0.020 ± 0.0017	46.52	4.65
800°C (80 cycles)	0.019 ± 0.0036	44.20	2.33
800°C (100 cycles)	0.020 ± 0.0012	47.30	5.43
1000°C (60 cycles)	0.022 ± 0.0027	51.17	9.30

Attempts were made to calculate the thickness of the affected layer after thermal shock, (see Figure 4.9 and Table 4.6). This was done by calculating the volume lost up to the time the curve of a heat treated sample converge with the non-heat treated sample. These calculations were done considering the convergence of the graphs in Figures 4.4 and 4.6. The differences in volume lost was translated into differences in affected layer thickness, see Table 4.6.

The results of these calculations show values which are not consistent with the results in Table 4.5. This suggests that the damaged layer was not of consistent thickness. This inconsistency will be explained in the next sections by analyzing the damaged layer using the microscopy. For 800°C (100 cycles) and 1000°C (100 cycles) the curves converge with the curve of the non-treated sample after 180 seconds, so no calculations could be done. This implies that at those conditions, the affected layer had not been removed completely after 180 sec.

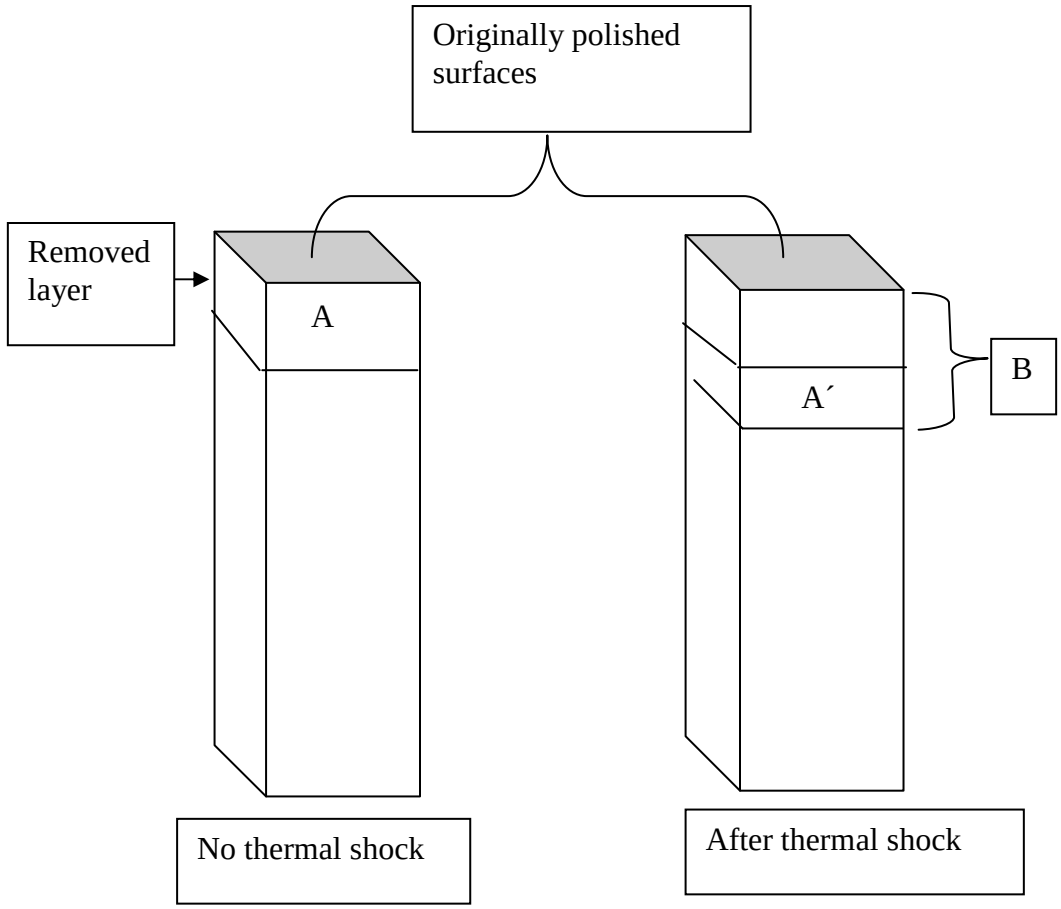


Figure 4.9: Schematic representation of the thickness of material removed during wear. A is the removed layer in samples without thermal shock and A´ is the removed layer which was not affected by thermal shock and thickness B – thickness A´ = affected layer by thermal shock.

Table 4.6: Mass loss at the time the curve of the heat treated samples converges with the curve of the non-heat treated samples and calculated affected layer.

	Mass loss at the convergence point (g)	Damaged thickness (µm)	Affected layer (µm)
No T.S (20°C)	0.015 ± 0.0015	35.59	0
600°C (60 cycles)	0.015 ± 0.0015	35.59	
No T.S (20°C)	0.017 ± 0.0015	39.54	2.33
800°C (60 cycles)	0.018 ± 0.0012	41.87	
No T.S (20°C)	0.0157 ± 0.0036	36.52	0.7
800°C (80 cycles)	0.016 ± 0.0012	37.22	
No T.S (20°C)	> 0.018 ± 0.001	> 41.87	#
800°C (100 cycles)	> 0.020 ± 0.0012	> 47.30	
No T.S (20°C)	> 0.018 ± 0.001	> 41.87	#
1000°C (60 cycles)	> 0.022 ± 0.0027	>5 1.17	

= Impossible to calculate because they converges after 180 sec.

However, after thermal shock the affected layers are expected to contain oxides, porosity and areas depleted of cobalt, therefore, the density should be lower than the original density of the sample and so the volume lost would be higher than the calculated values. This implies that the removed thicknesses calculated from heated samples are lower than the actual thicknesses, which suggest that the effect of thermal shock is larger than what is shown from Tables 4.4, 4.5, 4.6 and Figure 4.8.

4.2.4 SEM analysis of wear scars

This analysis was done to observe possible differences in the wear scars in samples exposed to different heat treatments. SEM micrographs were taken on samples after 180 seconds of abrasive wear. No obvious differences could be detected when comparing micrographs from different thermal shocks conditions. All the samples showed grooves, pits, and cracks on the WC grains, which are expected after abrasive wear. This may be because after 180 seconds of abrasive wear the wear rate was approximately the same for all the samples. Examples are shown in Figures 4.10 to 4.12. Arrows in all the micrographs indicate some of the wear features that where observed after abrasive wear.

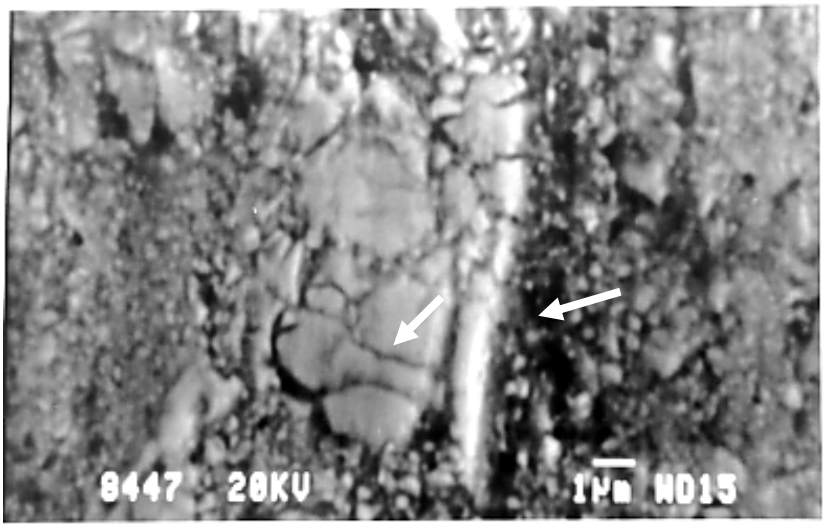


Figure 4.10: SEM micrograph after abrasive wear of WC-12wt%Co without thermal shock, showing grooves, pits and cracks that are perpendicular to the abrasive grooves.

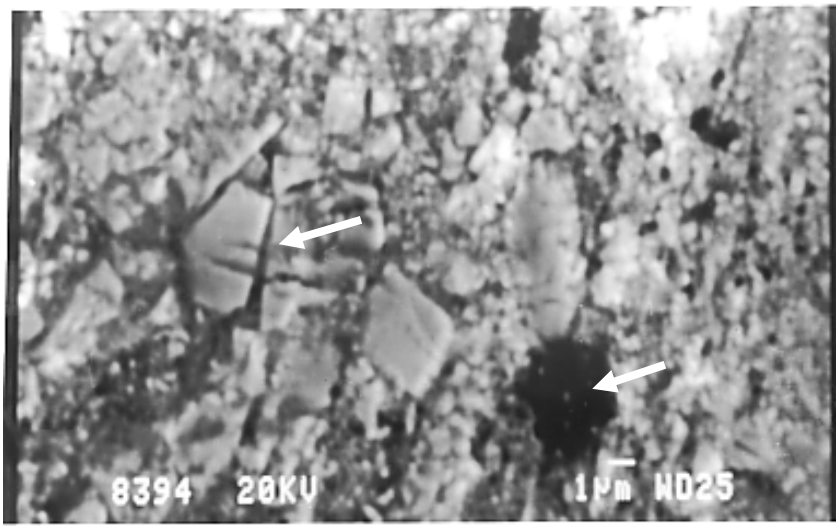


Figure 4.11: SEM micrograph after abrasive wear of WC-12wt%Co after 60 thermal shock cycles at 600℃ with similar features observed on sample without thermal shock.

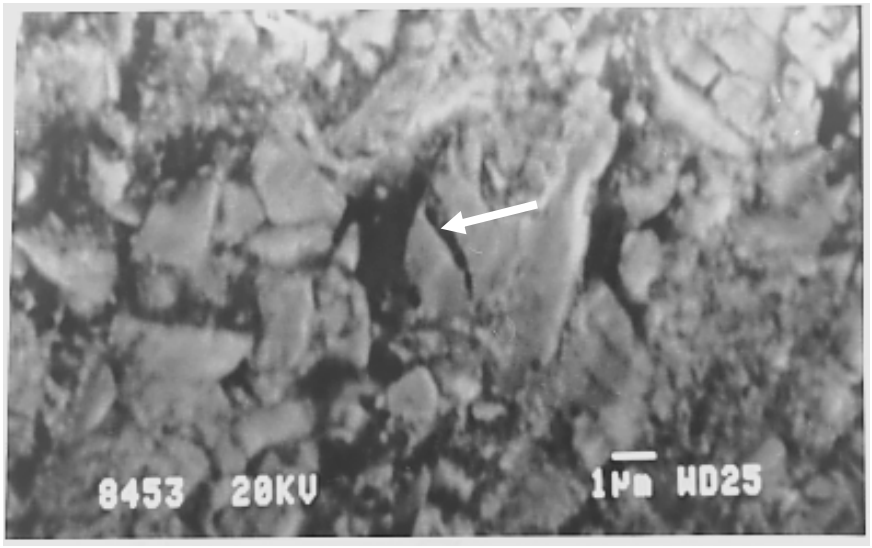


Figure 4.12: SEM micrograph after abrasive wear of WC-12wt%Co after 60 thermal shock cycles at 800℃ with similar features as observed in Figure 4.11.

4.3 Surface analysis

This section compares samples of WC-12wt%Co subjected to different thermal shocks to those not subjected to thermal shock starting from low to high magnification. As stated before two different thermal shocks routines where done i.e. varying the number of thermal shock cycles at constant temperature and varying the thermal shock temperature at a constant number of cycles (see Tables 3.1 and 3.2 in Chapter 3).

4.3.1 Surface analysis of samples subjected to thermal shock

Results on samples subjected to temperatures of 600°C, 800°C and 1000°C for 30 seconds in air then quenched in cold water are discussed in this section. The heat treatment was repeated 60 times at each temperature and 80 and 100 times at 800°C. Microscopic investigations of the surface layer showed that the cobalt was selectively removed and the surface appeared stained (see Figures 4.13 to 4.29). The depletion of cobalt was found to be random and this was confirmed by the EDS and microprobe analysis from all samples tested.

4.3.1.1 Effect of thermal shock temperature

The analyses were done using the stereomicroscopy. The surface of the samples (which was originally polished) became discolored after thermal shock i.e. the surface appears stained. The discolourization increased as the temperature increased. The surfaces are shown in the stereo-micrographs in Figures 4.13 to 4.16. The concentric

marks on the surface could be water marks which formed when the sample was heated up again; this is because during thermal shock procedure, the samples where not dried up for the next thermal shock cycle.

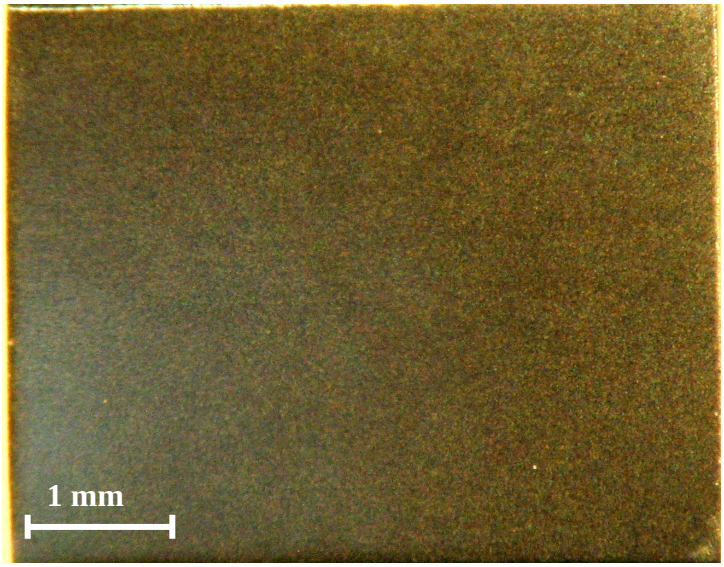


Figure 4.13: Micrograph of WC-12wt%Co before thermal shock.

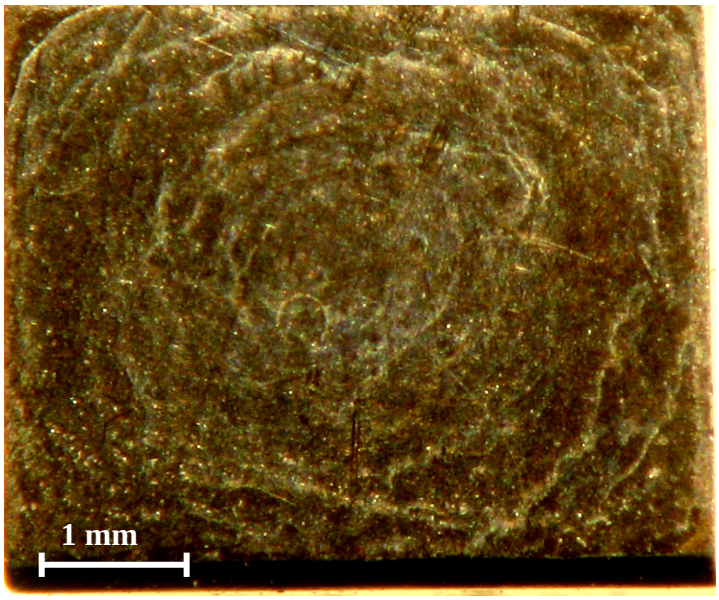


Figure 4.14: Micrograph of WC-12wt%Co after series of 60 cycles of thermal shock at 600°C showing concentric marks around the middle of the specimen.

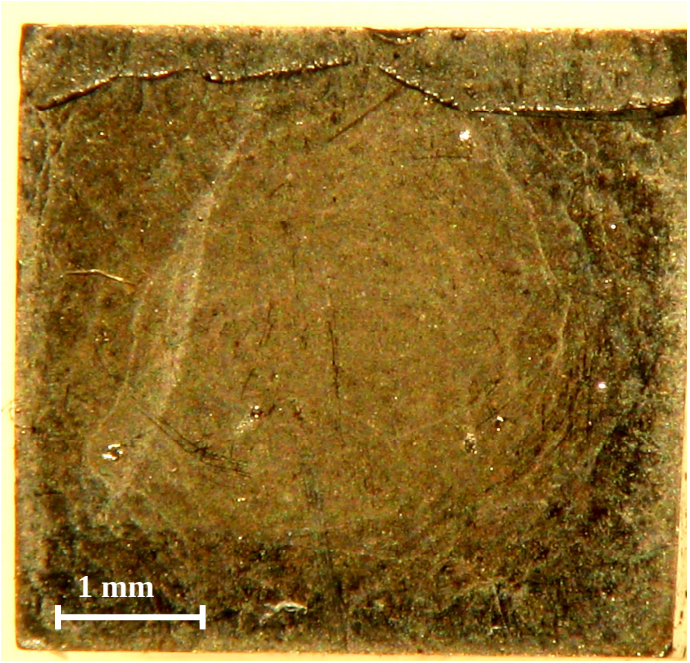


Figure 4.15: Micrograph of WC-12wt%Co after 60 cycles of thermal shock at 800°C.

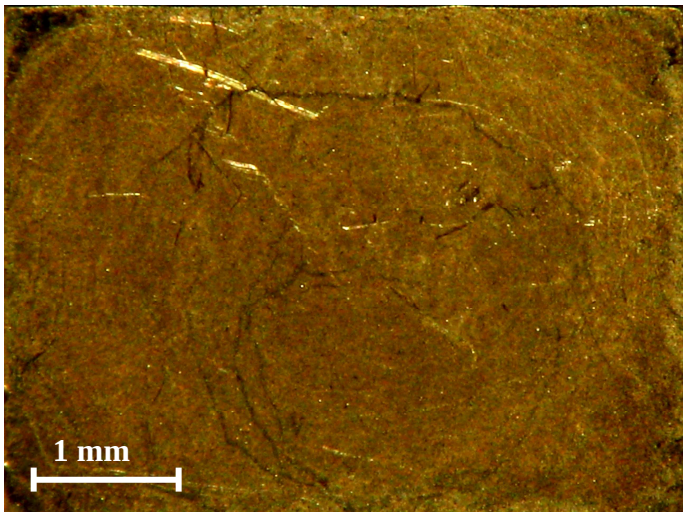


Figure 4.16: Micrograph of WC-12wt%Co after 60 cycles of thermal shock at 1000°C.

Figure 4.15 and 4.16 shows dark lines that appear to be fine cracks on the surface of the sample. This is an indication of surface cracks due to thermal shock as was also observed by most of the authors discussed in Chapter 2.

60 cycles of thermal shock at 600°C

Figure 4.17 (a) and (b) are SEM micrographs taken at the centre and the edge of the sample. Figure 4.17 (b) shows white spots on the surface of the material, which appear to be particles. See section 4.3.2.1 for analysis on the white spots.

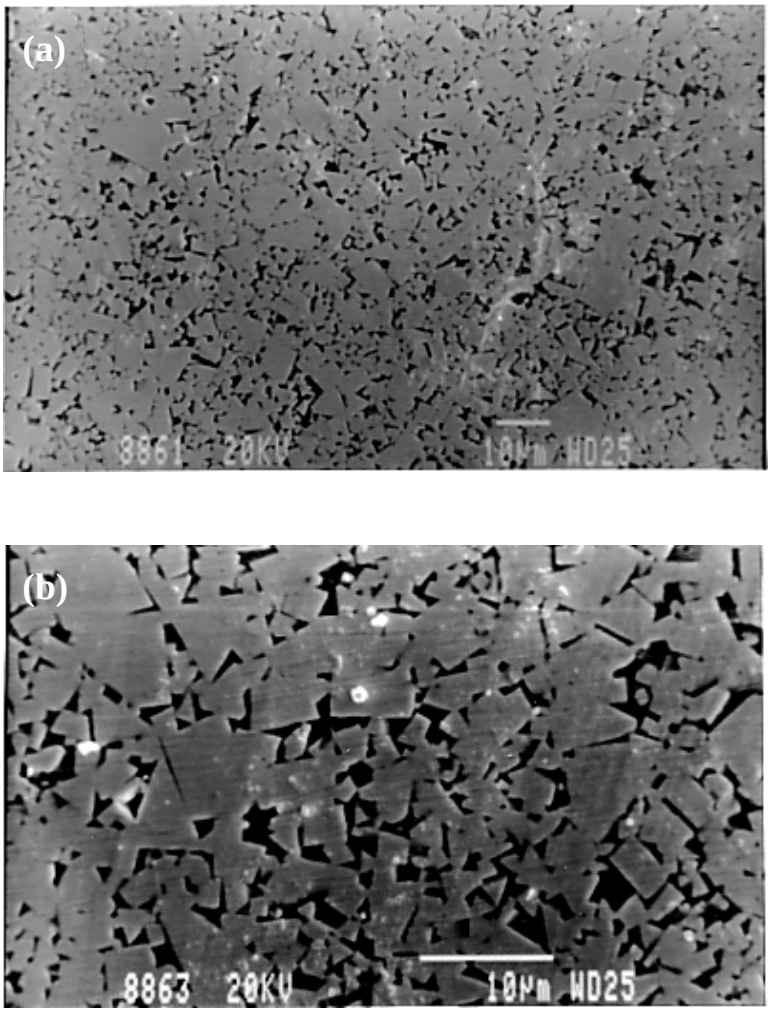


Figure 4.17: SEM micrographs of sample subjected to thermal shock for 60 cycles at 600°C, (a) micrograph near the edge, (b) micrograph at the centre.

60 cycles of thermal shock at 800°C

Circled areas in Figure 4.18 (a) and (b) indicate regions of random cobalt removal. These random removals of cobalt were confirmed using the EDS (see Section 4.3.2.2). The white spots shown in Figure 4.17 were also observed in this thermal shock condition and appeared to be more at the centre than the edge. The reason for having white spots more in the centre is not known. See Figure 4.19 (a) and (b).

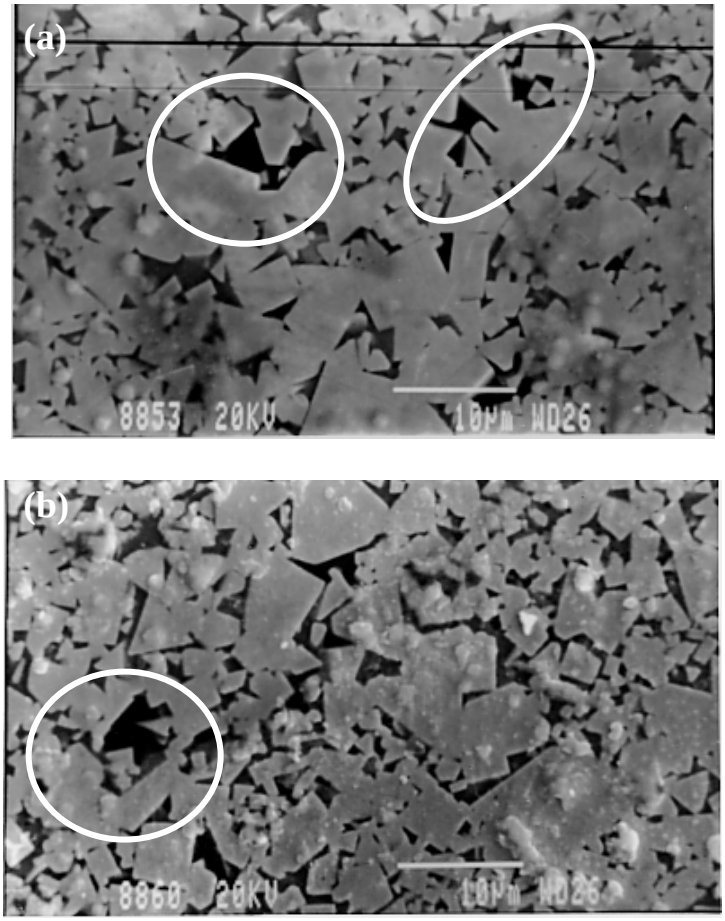


Figure 4.18: SEM micrographs of sample subjected to thermal shock for 60 cycles at 800°C. (a) Shows voids and the black horizontal line is a charging effect in the SEM, (b) shows cobalt depletion and white spots.

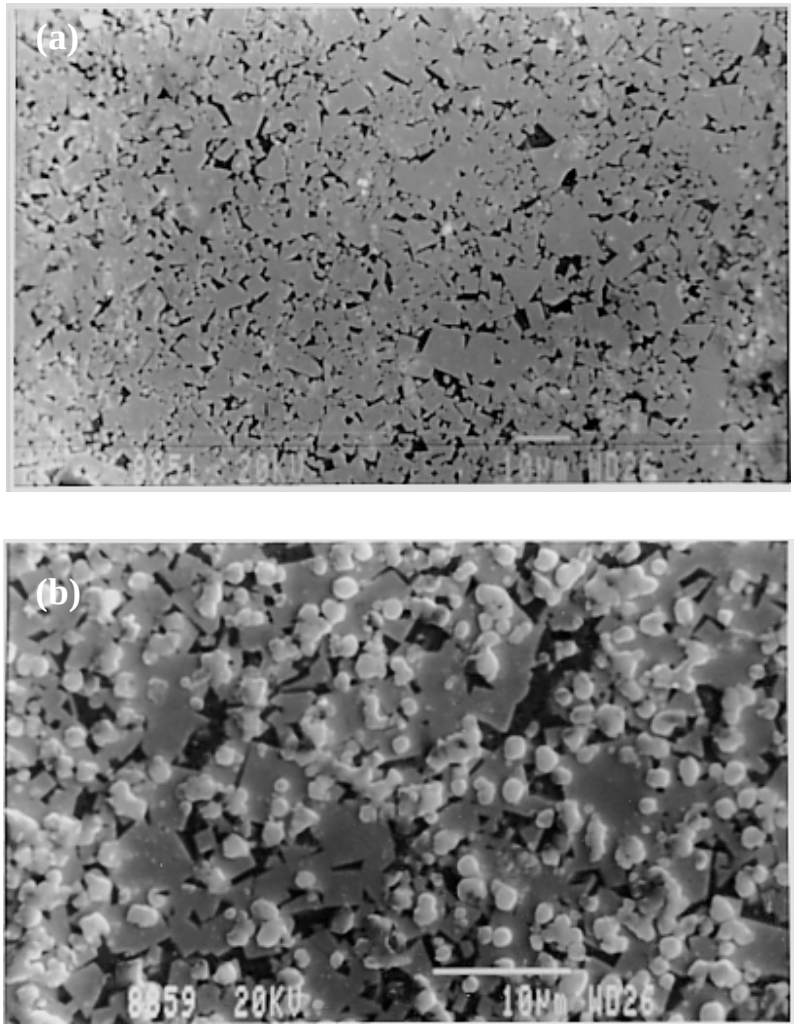


Figure 4.19: SEM micrographs of sample subjected to thermal shock for 60 cycles at 800°C, (a) near the edge of the surface with less white particles, (b) taken at the centre. It shows white round spots covering the surface which are particles.

60 cycles of thermal shock at 1000°C

The main difference between this test and the rest of the tests is that the microstructure was difficult to see, since almost the whole surface was covered with white particles, see Figures 4.20 and 4.21. A blue colour was observed during and after the tests in this thermal shock condition. The colour change suggests the formation of an oxide layer on the surface.

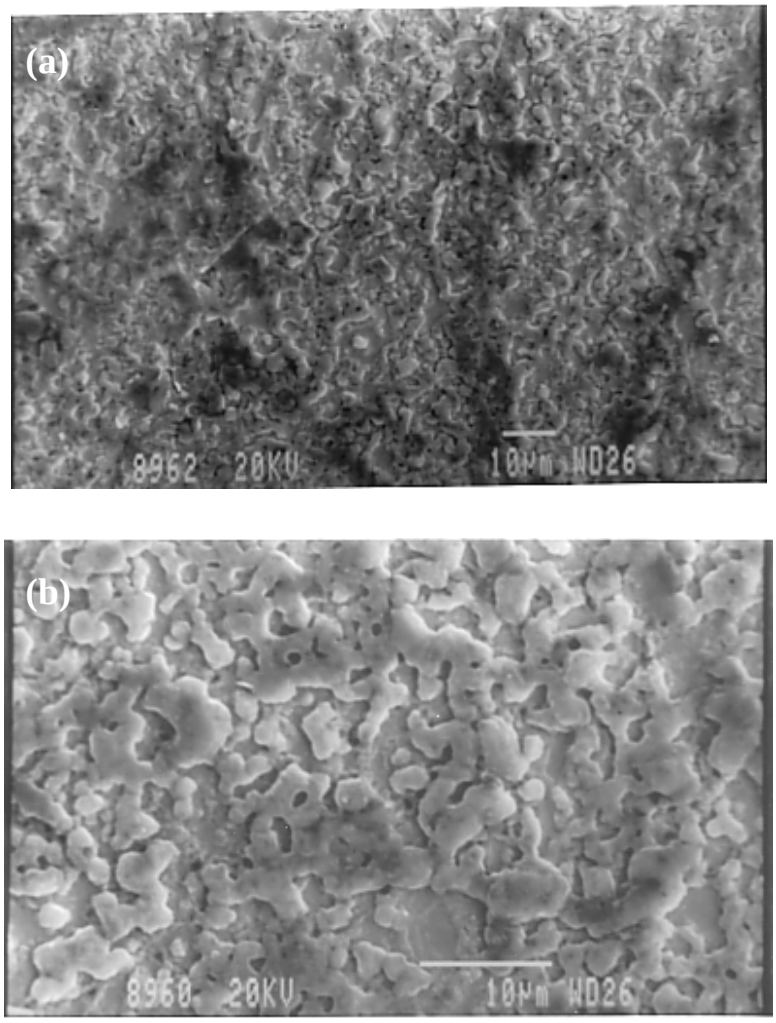


Figure 4.20: SEM micrographs of sample treated at 1000°C for 60 cycles a) is covered with a layer b) closer view showing that the layer appears to consist of a high density of white particles, joined to each other.

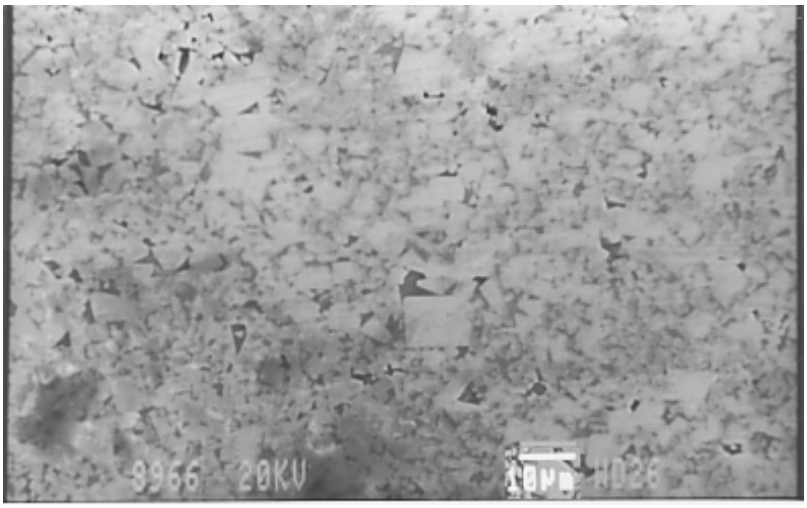


Figure 4.21: Micrograph of one of the areas of the sample treated at 1000°C for 60 cycles where less white spots were detected, mainly near the edges. This micrograph shows a thin covering layer that reduces the visibility of the microstructure.

Summary

Random voids between the WC grains appeared in all the tests but fewer found at 60 cycles of thermal shock at 600°C i.e. at the lowest thermal shock temperature. The density of the white particles and the discolorization observed on the surface increased when increasing the heating temperature. Mining industries do not use 100% clean water to flush away crushed rocks during drilling. Therefore it is possible that the water used may contain foreign elements like calcium. Thus the formations of white particles or other chemical reaction products are possible; see Section 4.3.2.2 for further analysis on white particles. Feint surface cracks are observed in this investigation and were also observed by other authors quoted in the literature review [2]. The voids might have been generated in the same way the surface cracks are generated, i.e. differences in contraction between the interior and the surface of the material or different thermal expansion behaviour between the WC and the Co resulting in the Co to vacate to the surface.

4.3.1.2 Effect of thermal shock cycles

Samples are compared after thermal shock when varying the thermal shock cycles (60, 80, and 100 cycles) at a heat treatment temperature of 800°C (see Figures 4.22 to 4.24). These micrographs where acquired using the stereomicroscopy. As the thermal shock cycles increased, discolorization of the surfaces increased but to a lesser degree than when varying the heating temperatures.

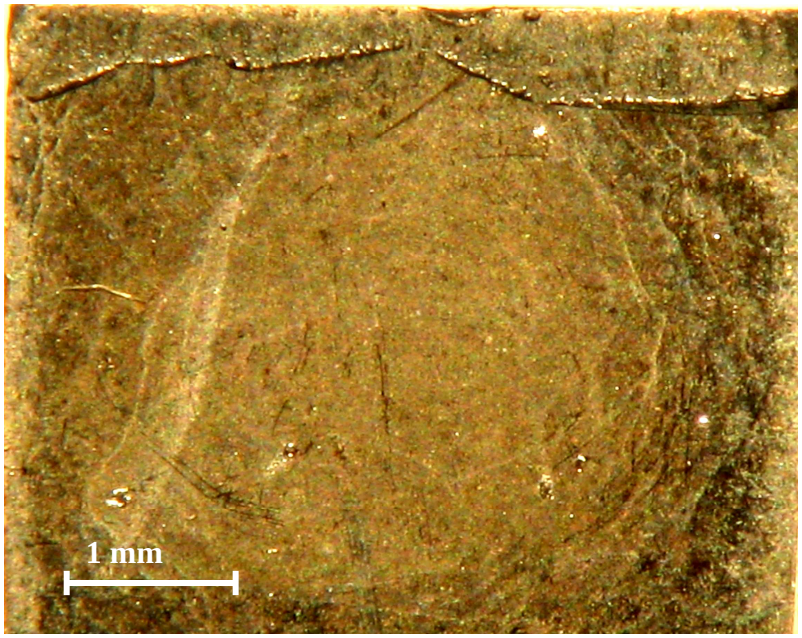


Figure 4.22: Micrograph of WC-12wt%Co after 60 thermal shock cycles at 800°C. Details of this thermal shock condition where presented in section 4.3.1.1.

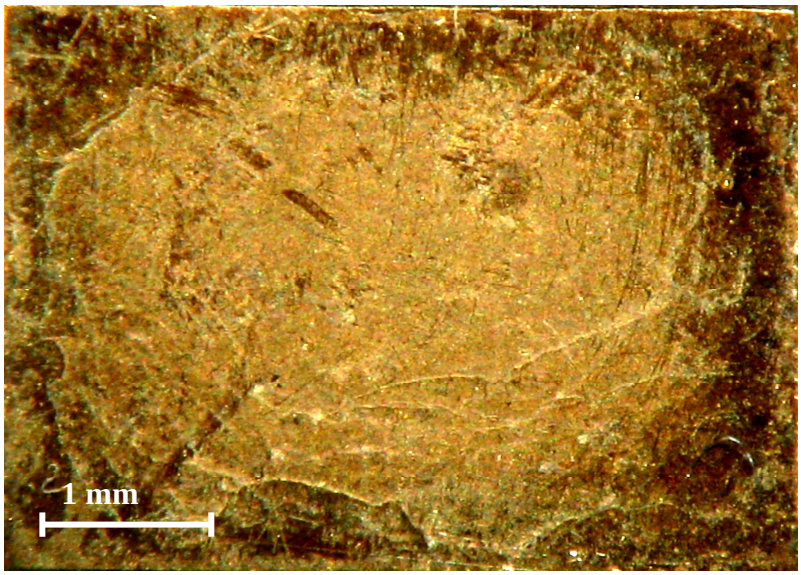


Figure 4.23: Micrograph of WC-12wt%Co after 80 thermal shock cycles at 800°C.

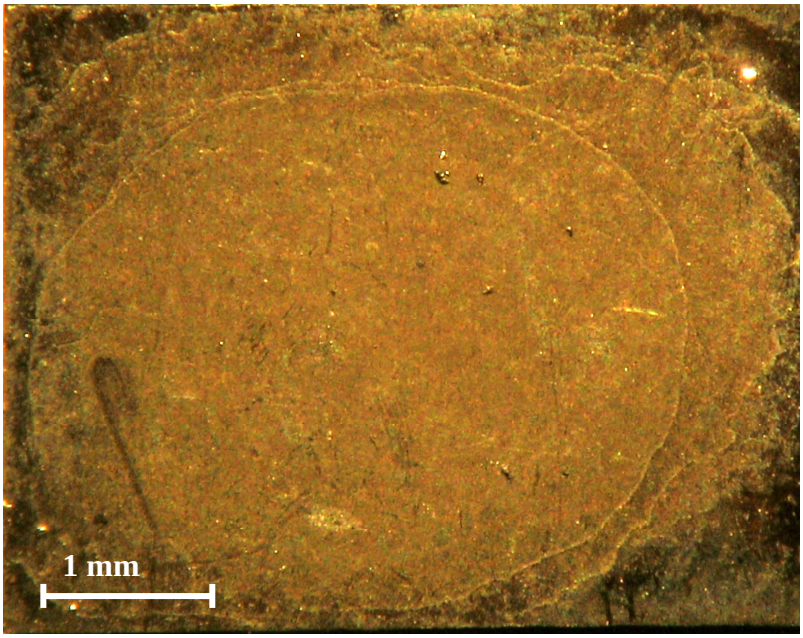


Figure 4.24: Micrograph of WC-12wt%Co after 100 thermal shock cycles at 800°C.

60 cycles of thermal shock at 800°C

The features observed on these samples have already been described in section 4.3.1.1.

80 cycles of thermal shock at 800°C

The degree of discolouration increased compared to some of the previous tests discussed (60 cycles of thermal shock at 600°C and 60 cycles of thermal shock at 800°C). Areas of cobalt removal, which are now in clusters, can be seen in Figures 4.25 and 4.26(a). Figure 4.26(b) shows white particles on the surface which were observed mostly in the centre of the specimen.

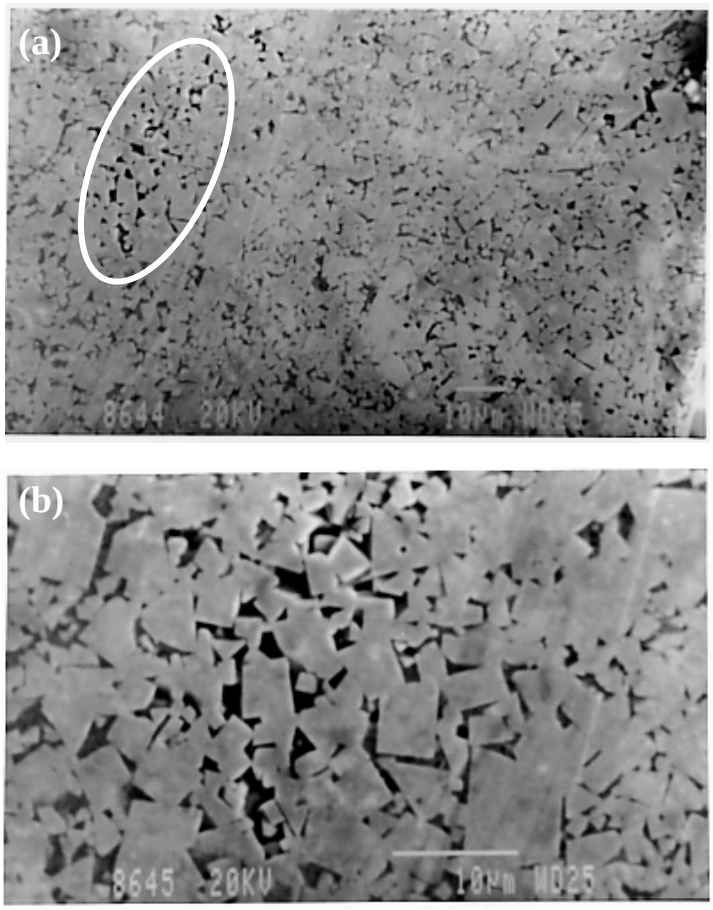


Figure 4.25: SEM micrographs (near the edge) of the WC-12wt%Co sample after being subjected to 80 cycles of thermal shock at 800°C. Cobalt has been selectively 'removed' from the alloy surface. The circled area in (a) is shown at high magnification in (b).

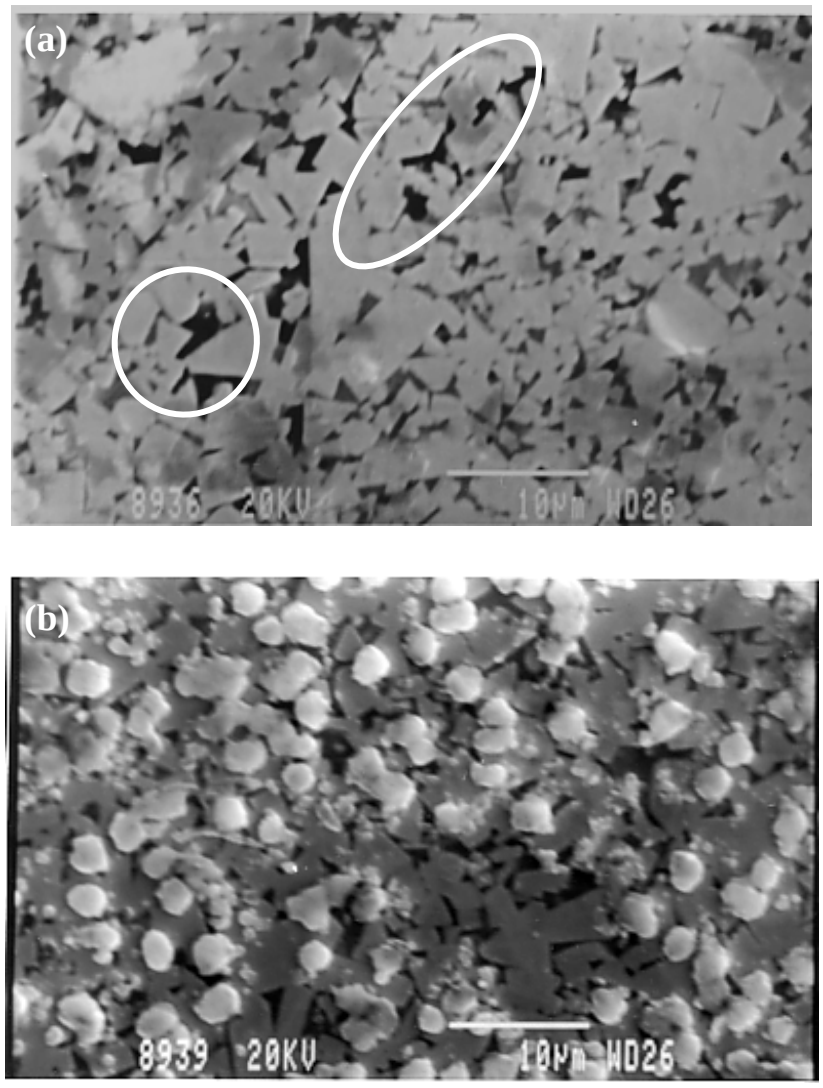


Figure 4.26: SEM micrographs of sample treated at 800°C for 80 cycles, a) is taken near the edge with clusters of voids between the WC grains b) taken in the middle of the specimen with white particles.

100 cycles of thermal shock at 800°C

The same cobalt depletion and white particles were observed as previously described with a higher concentration of white particles covering the surface, refer to Figure 4.27 and 428.

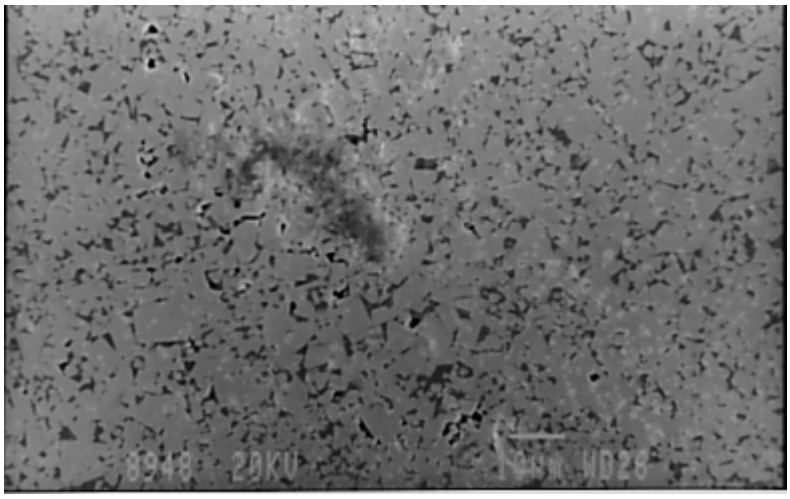


Figure 4.27: SEM micrograph from near the edge of the surface of a WC-12wt%Co sample after being subjected to thermal shock at 800ºC for 100 cycles.

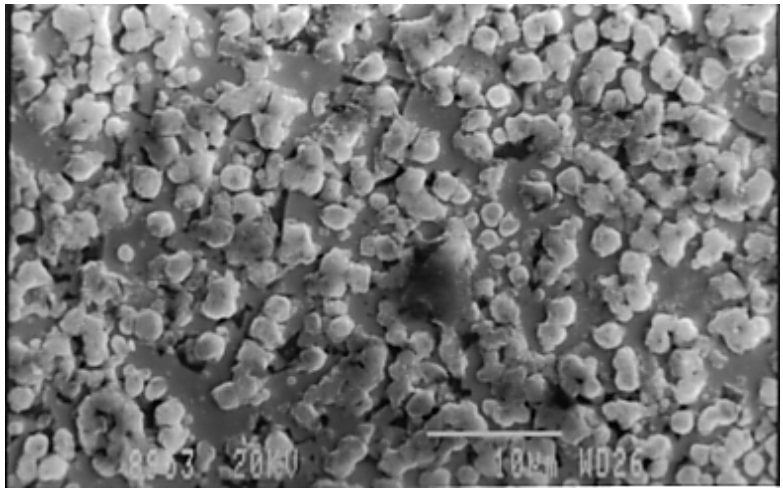


Figure 4.28: SEM micrograph showing white particles containing calcium observed in the middle of the sample.

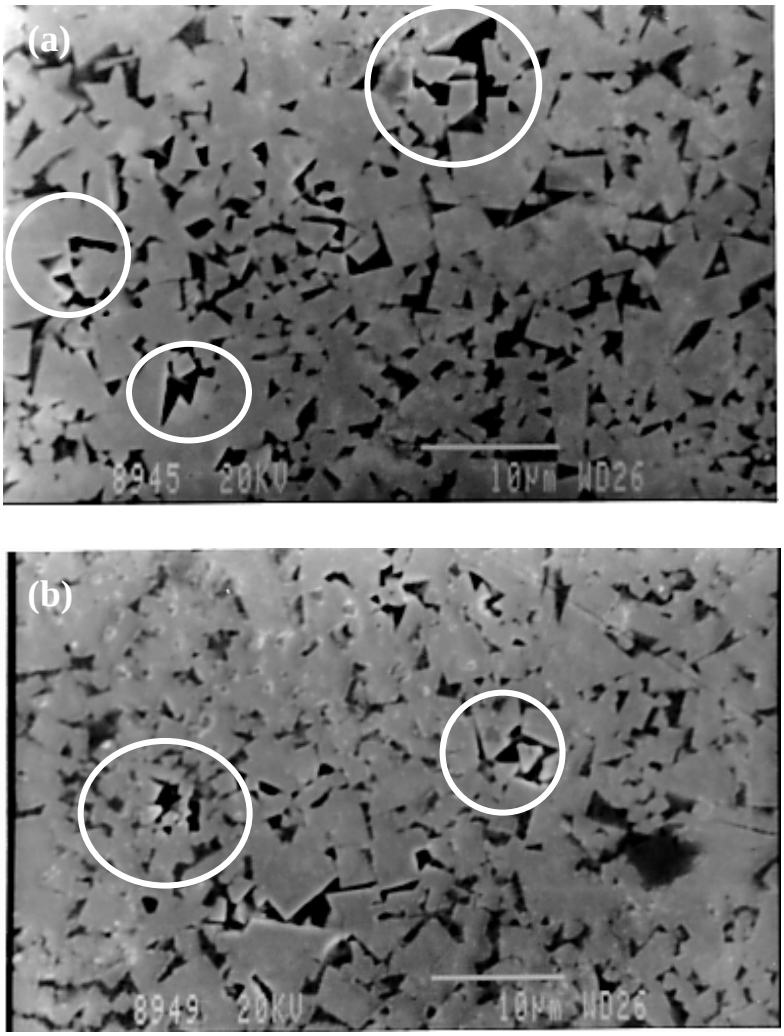


Figure 4.29: SEM micrographs of sample treated at 800°C for 100 cycles near the edge. (a) Shows voids between the WC grains, in some areas in (b) some of the grains are covered with a thin layer.

Random voids and centralised white particles on the surface where also observed when varying the thermal shock cycles but it is difficult to say if the density varied. Figure 4.29 (b) showed a thin layer covering the grains, which may be a stain, or an oxide layer. The other interesting observation was the centralised white particles observed on the surface.

4.3.1.3 Surface Oxidation

The next investigation was the possibility of oxide formation as samples of WC-12wt%Co where subjected to temperatures of 600°C, 800°C and 1000°C. Other authors observed oxidation on WC-Co at temperatures as low as 500°C with only two oxides forming at temperatures ranging from 500°C to 1000°C, namely WO_3 and $CoWO_4$ [23-25].

EDS analysis revealed oxygen on the surface of all the samples after thermal shock (see Figure 4.30). This suggests possible oxide formation. No oxygen peaks where observed on cross-sections of samples after thermal shock far from the surface, as shown by EDS in section 4.3.3.

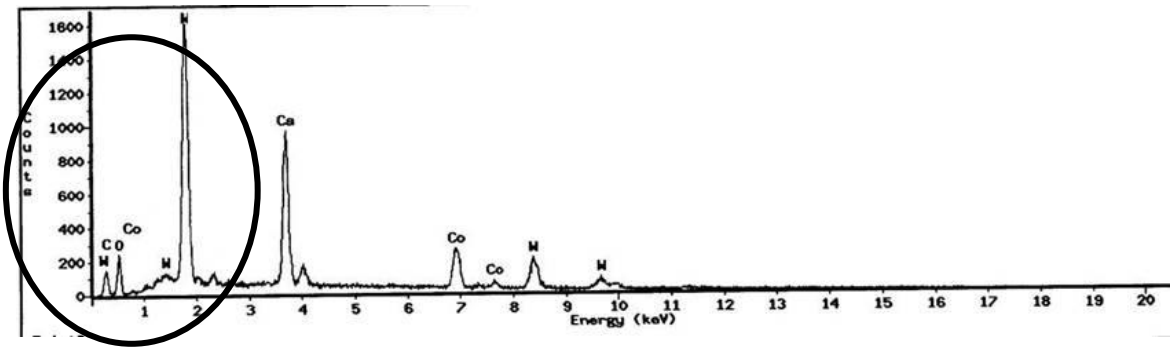
The mass of WC-Co is known to change as oxidation increases [31]. This section reports if and how the mass changed as a result of thermal shock possibly due to oxide formation. Table 4.7 lists the mass change of WC-12wt%Co from before to after thermal shock.

Table 4.7: Mass change of samples after thermal shock.

	Mass before (g)	Mass after T.S(g)	Differences (g)
600°C-60cycles	4.526	4.526	——
800°C-60cycles	3.865	3.865	——
800°C-80cycles	4.357	4.357	——
800°C-100cycles	4.133	4.135	↑ 0.002
1000°C-60cycles	4.257	4.268	↑ 0.011

This table shows only a slight increase in mass after 60 thermal shock cycles at 1000°C and 100 thermal shock cycles at 800°C. This suggests the presence of a possible thin oxide layer after those tests. At 800°C-100 cycles the test showed that a little oxidation occurred with the mass increase of 0.002g while there was no mass increase at 800°C-60 and 800°C-80 cycles. Therefore the thin layer that was observed on the SEM after 100 cycles at 800°C and 60 cycles at 1000°C (see Figures 4.21 and 4.29) was probably a layer of oxide.

Figure 4.31 shows an experiment carried out to confirm the formation of oxide. A sample of WC-12wt%Co was subjected to 20 thermal shock cycles at 800°C; the sample was heated for 5 minutes at each cycle. Figure 4.31 B and D show a blue oxide layer of WO_3 covering the whole surface with a considerably high shape change when compared to the original sample. The change of shape observed was due to oxide formation and swelling of the new phase which occurs at areas of high stress concentration [26].



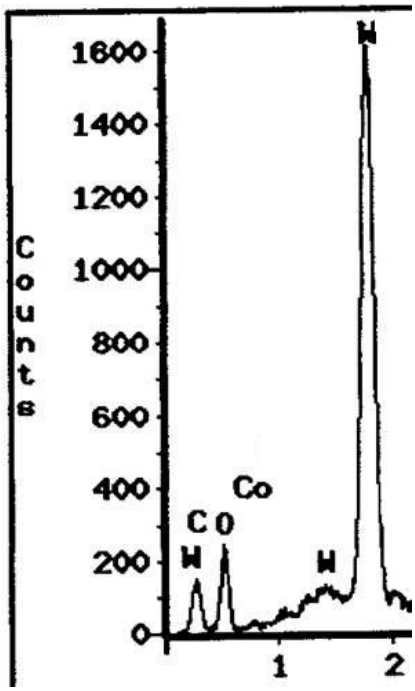


Figure 4.30: EDS spectrum of a sample subjected to 60 cycles of thermal shock at 1000 ℃. The spectrum shows an oxygen peak, suggesting the presence of oxides.

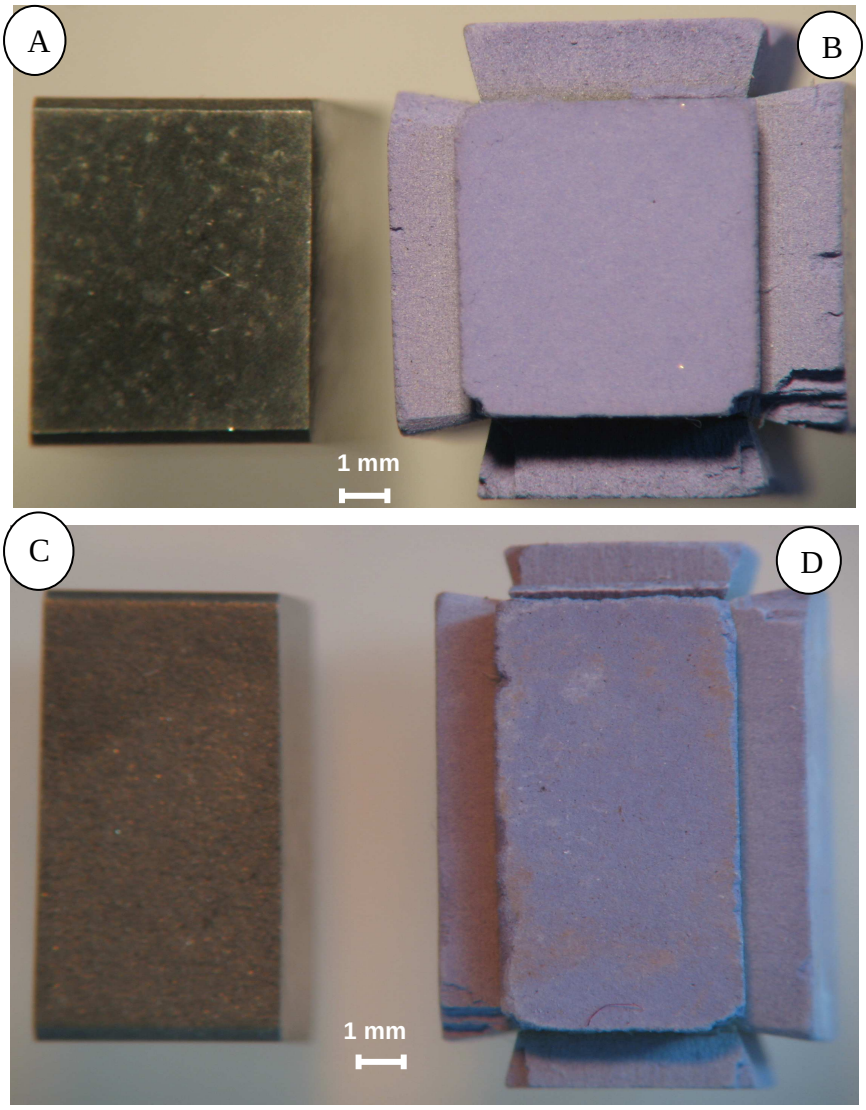


Figure 4.31: Shape change of a rectangular sample of WC-12wt%Co after 20 thermal shock cycles at 800℃ of 5 minutes each. A and B are the top views while C and D are the side views. A and C shows the initial shape of the sample i.e. before thermal shock, while B and D represent the shape after thermal shock.

The oxide layer was found to be approximately 2mm thick and the weight of the sample increased considerably after thermal shock. The measurements were approximated using a ruler after removing one side of the oxidized layer to have a clear view of both. i.e. non-oxidized solid block and oxidized layer. The original size

of the specimen was 10×5×6 mm plates, implying that only a small solid block was left non-oxidized after thermal shock.

4.3.1.4 Crack formation on the surface

Previous investigations by other authors showed that surface cracks are formed during the drilling operation as a result of thermal shock [2,23,24]. Some of the surface cracks are called snake skin or reptile skin cracks. These cracks can lead to catastrophic fracture [2].

In this investigation no clear surface cracks were observed which suggests that the cracks can be nucleated only by numbers of heating cycles much larger than those carried out in this investigation or maybe the thermal shock procedure followed in this project was insufficient. However some faint surface cracks are reported here.

Figures 4.32 and 4.33 show the surface cracks that were found after the tests. These were observed in all the tests done: 600°C for 60 cycles, 800°C for 60,80,100 cycles and 1000°C for 60 cycles. It was reported after investigating the micrographs below that the cracks prefer to propagate through the binder phase or along the WC grain boundary. Cobalt is tough and less hard compared to the WC, which could make it the weakest link during crack formation.

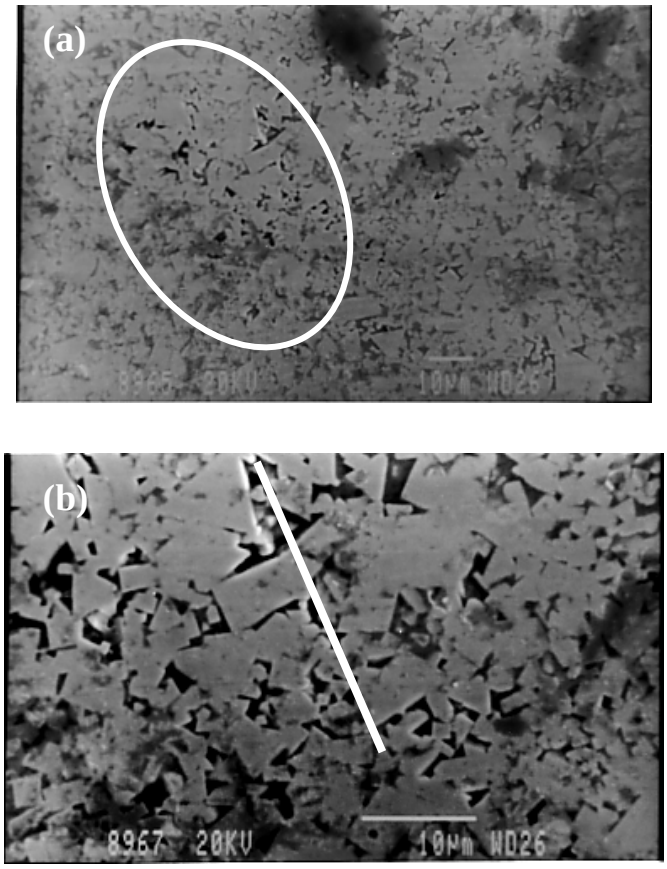


Figure 4.32: Voids on WC-12wt%Co after thermal shock. The circled area in (a) is shown at high magnification in (b). The white line shows the direction of what could possibly be feint crack.

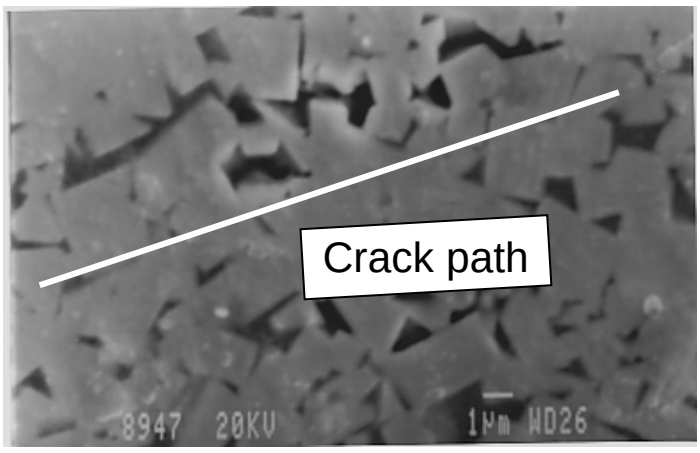


Figure 4.33: Voids on the surface of a thermally shocked sample, with path parallel to the white line.

4.3.2 EDS analysis

These tests were done to confirm the cobalt depletion and to identify the white particles observed when investigating the surfaces described in section 4.3.1.1 and 4.3.2.2. Figures 4.34 to 4.36 show the microstructure and the EDS spectra of WC-12wt%Co without thermal shock.

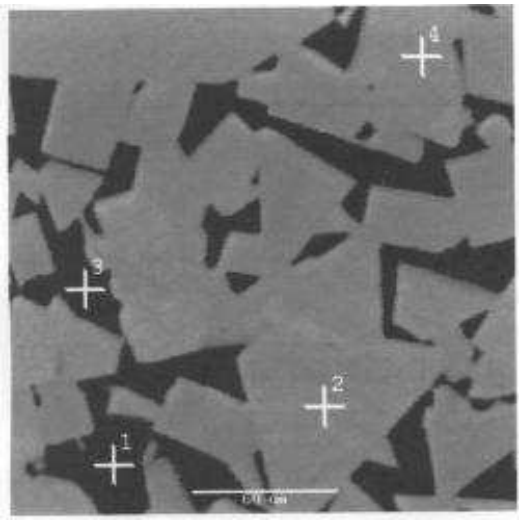


Figure 4.34: SEM micrograph of WC-12wt%Co without thermal shock with numbers on the grains corresponding to the EDS spectra in figures 4.35 and 4.36. Spots 1 and 3 are expected to have spectra with high Co peaks and spots 2 and 4 with high WC peaks.

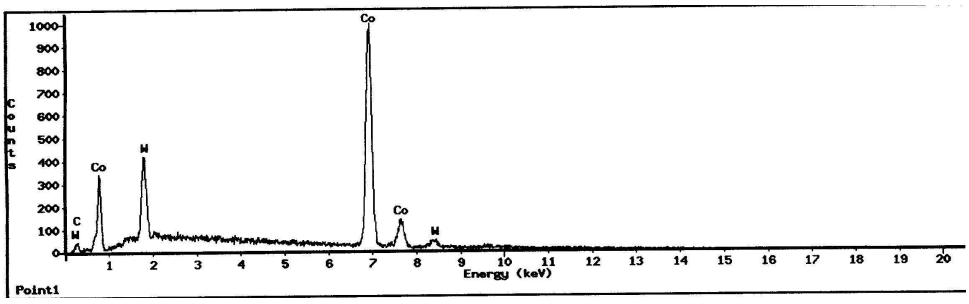


Figure 4.35: EDS spectrum of spot 1 in Fig. 4.34 showing a high Co peak. Spot 1 and 3 showed the same spectrum peaks.

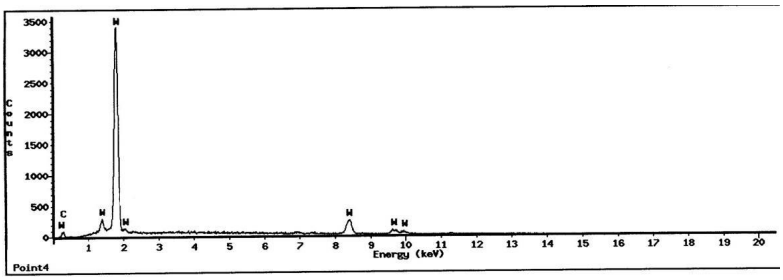


Figure 4.36: EDS spectrum of spot 4 with high a W peak. The grey angular particles are hard WC grains and the dark material between the WC grains is cobalt (See figure 4.34).

4.3.2.1 Cobalt removal

Random removal of cobalt caused by thermal shock was investigated by using the EDS spot analysis. This cobalt depletion was observed in all the tests, i.e. varying the thermal shock temperature and varying the thermal shock cycles. Figures 4.37 to 4.39 confirm that there is random missing cobalt in between the WC grains.

Regardless of all this analysis, the spot EDS is not very conclusive as it can detect phases that are overlapping, and interacting phases deep in the specimen can also be detected

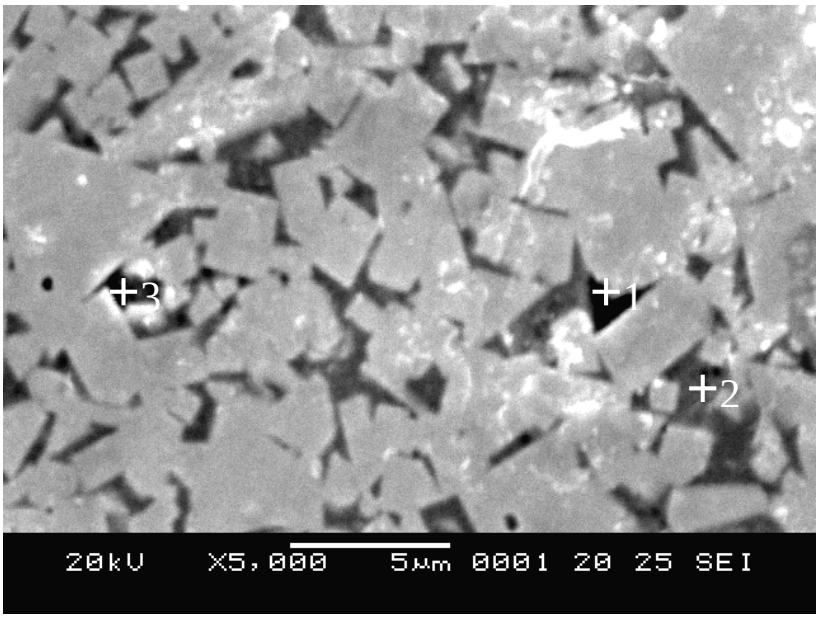


Figure 4.37: SEM micrographs of WC-12wt%Co after 60 thermal shock cycles at 1000°having spot numbers corresponding to the spectra in Figures 4.45 and 4.46.

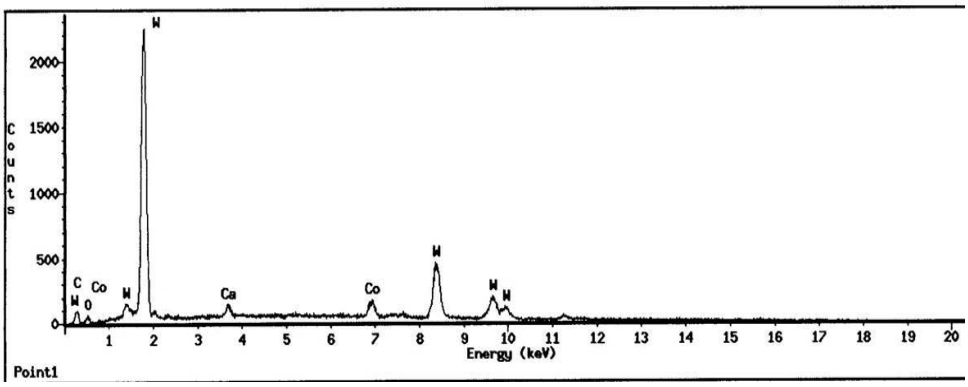


Figure 4.38: EDS spectrum of spot 1. The spectrum shows a large amount of W in and around the void with a low cobalt peak. This implies that cobalt binder has been removed.

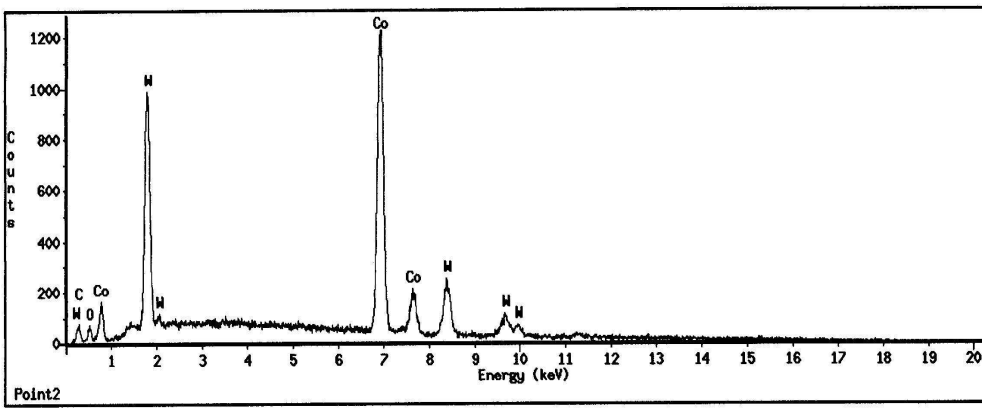


Figure 4.39: EDS spectrum of spot 2. The spectrum shows a large amount of Co. This was expected because the spot is mostly on the Co binder and partly on the WC grains.

4.3.2.2 White particles observed after thermal shock

The white particles reported in sections 4.3.1.1 and 4.3.1.2 where analyzed using the EDS. Peaks of calcium were found in the EDS spectra from the surface of the samples. The calcium was probably in solution in water [39], and that water containing calcium was used for quenching. Spot and area analysis on the surfaces was done to understand this calcium formation (see Figures 4.40 and 4.41).

The samples of WC-12wt%Co were heated to 600°C, 800°C and 1000°C, and then quenched in room temperature water. The water surrounding the surface of the samples must have boiled immediately on contact with the sample since the boiling temperature of water is 100°C, i.e. very low compared to the temperature of the samples, as the water boiled it produced bubbles of water vapour. While the water vapour found its way out of the water, the calcium in solution precipitated on to the surface of the samples when the water vaporized [39]. This may explain the increase of white particles with increasing temperature because the boiling of water at the

surface and the formation of bubbles must have been more intense at higher temperatures (see Figures 4.42 to 4.46). Figure 4.40 shows an area that was analyzed at four spots.

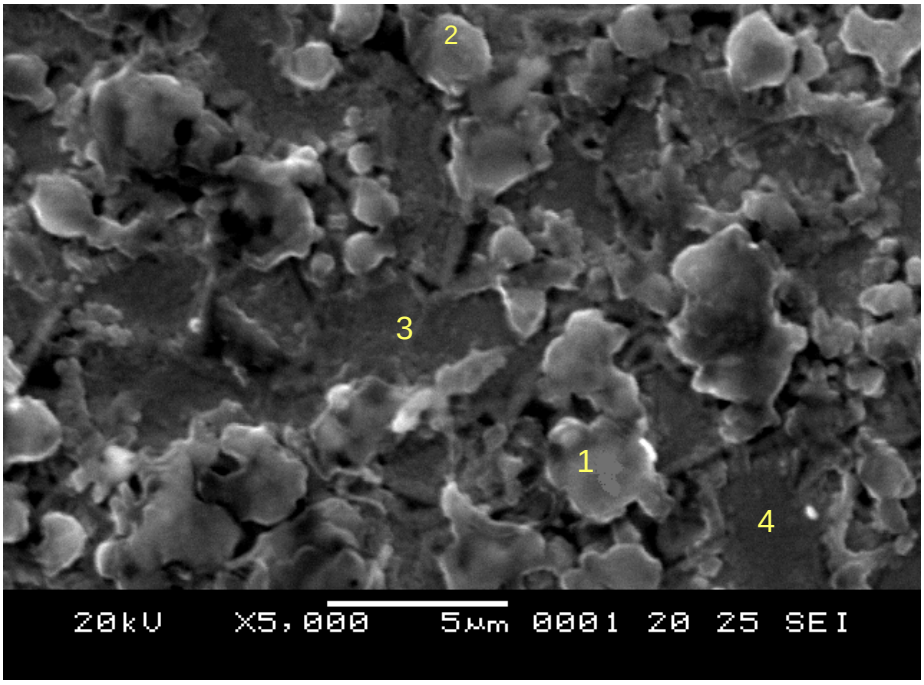


Figure 4.40: SEM micrograph of WC-12wt%Co after 60 thermal shock cycles at 1000°C showing white spot formation.

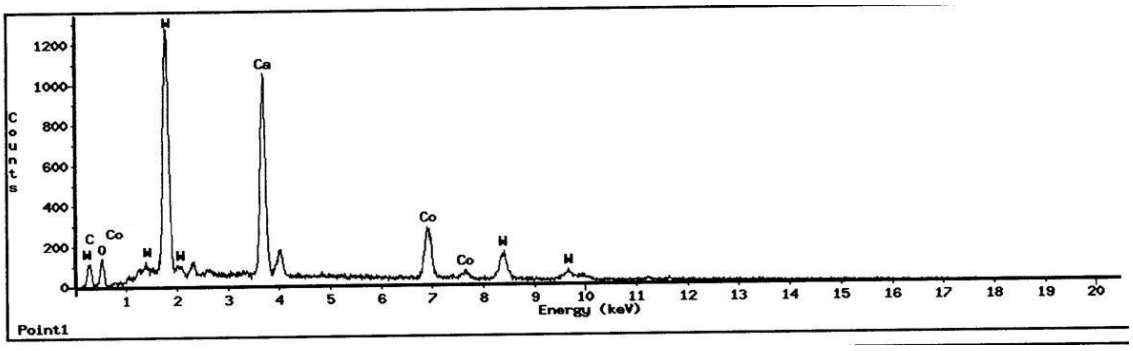


Figure 4.41: EDS spectrum of spot 1, Ca, Co and W peaks are visible.

Spot 2 of Figure 4.40 gave a similar spectrum as in Figure 4.41. Spot 3 and 4 in Figure 4.40 showed high peaks of W with no Ca and Co peaks. Area EDS analysis were also done on the samples after thermal shock to compare the peaks of calcium. The comparisons were done on the thermal shock temperature and the number of thermal shocks increases. The EDS spectra show that, the calcium peaks increase as the thermal shock temperature increases (see Figures 4.42, 4.43 and 4.46). However the same cannot be said for varying the thermal shock cycles at 800°C as the spectra show peaks of calcium of equal intensity at 60, 80 and 100 cycles of thermal shock (see Figures 4.43-4.45).

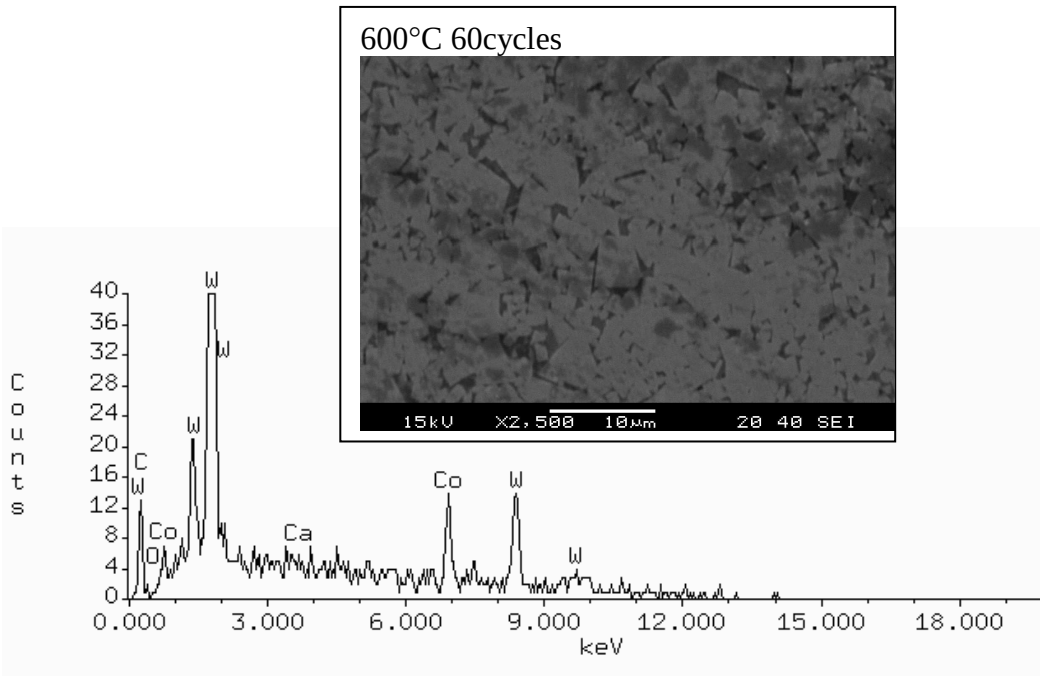


Figure 4.42: EDS spectrum of sample after 60 cycles of thermal shocks at 600ºC.

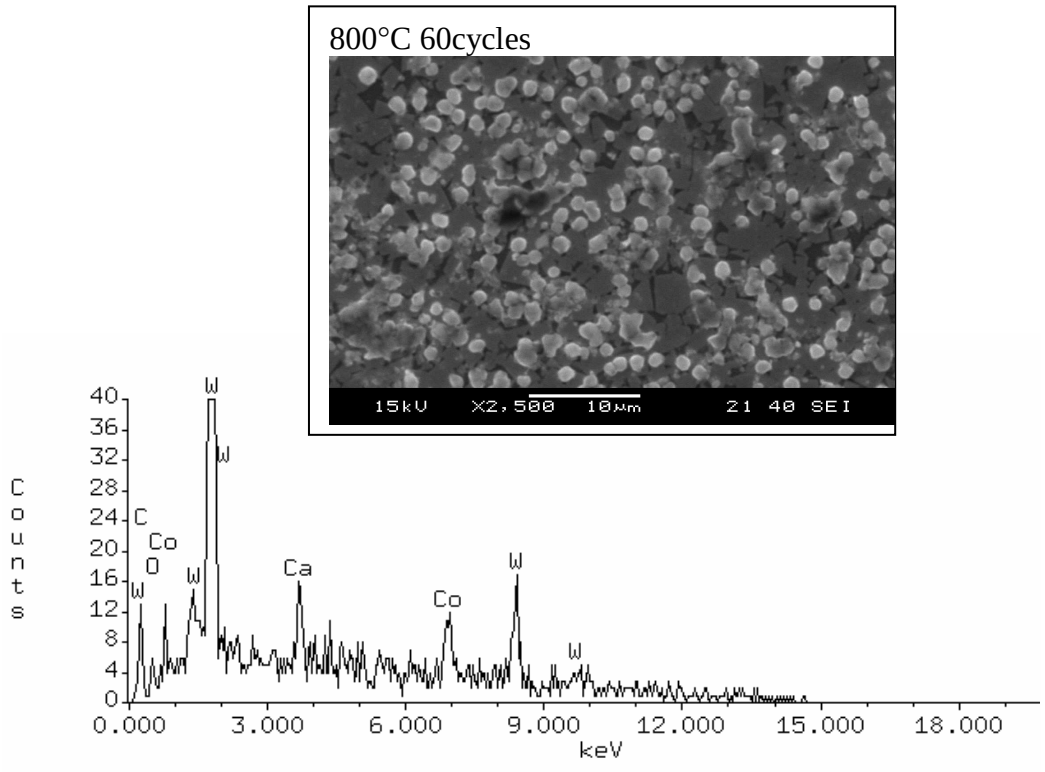


Figure 4.43: EDS spectrum of sample after 60 cycles of thermal shocks at 800ºC.

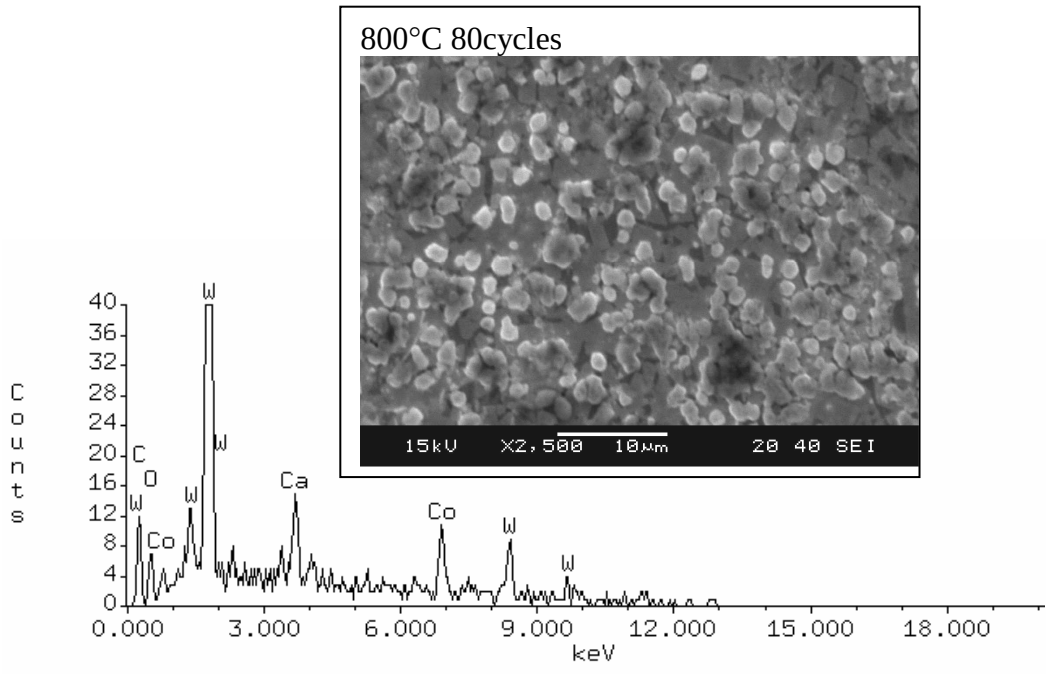


Figure 4.44: EDS spectrum of sample after 80 cycles of thermal shocks at 800ºC.

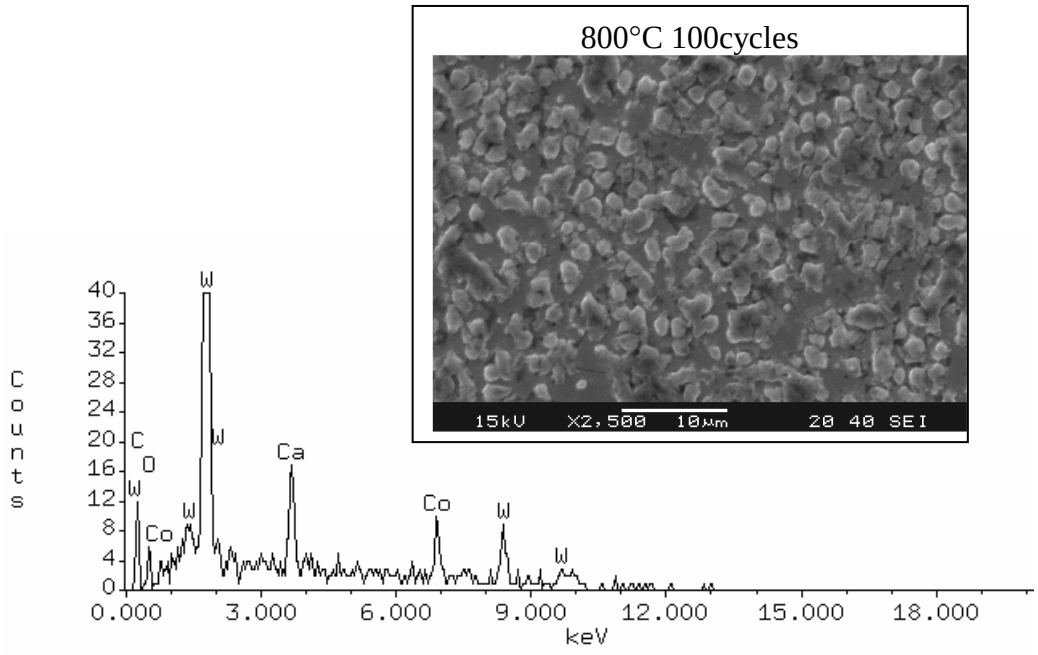


Figure 4.45: EDS spectrum of sample after 100 cycles of thermal shocks at 800ºC.

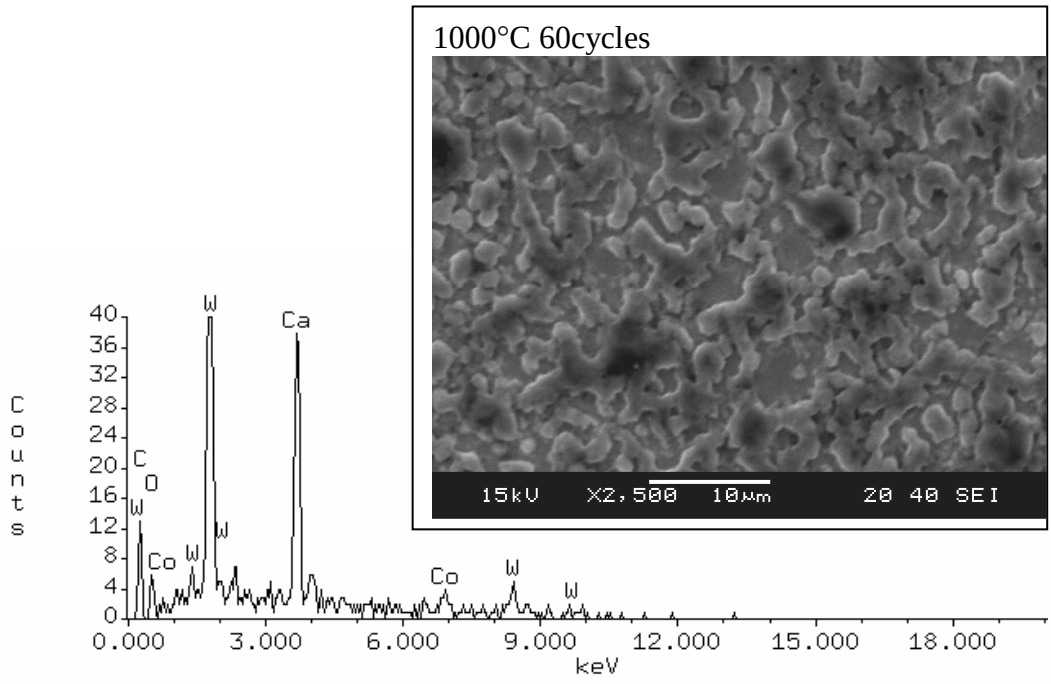


Figure 4.46: EDS spectrum of sample after 60 cycles of thermal shocks at 1000ºC.

These spectra show an interesting observation of oxygen peak being lower than the Co peak after 60 cycles at 600ºC and 800ºC but became higher after 80 and 100 cycles at 800ºC and 60 cycles at 1000ºC. This observation suggests increasing oxidation with increasing temperature.

4.3.3 Analysis of cross-section

The cross-sections of all samples were analyzed to assess the depth of the surface damage done by thermal shock. Some authors observed cracks on cross-sectional polished samples after thermal shock and wear [3, 16].

4.3.3.1 Cobalt depletion

Figures 4.47(a) to (c) are SEM micrographs revealed a possible removal of binder phase along the edges of the samples subjected to 60 thermal shock cycles at 600°C and 800°C. This is consistent with evidence from the abrasive wear graphs in section 4.2 where the damaged edges observed here may have accelerated the wear rate only at the beginning of the tests. An oxide layer at the surface of the specimen would be brittle and porous and could therefore be easily removed during wear as it was the case in Section 4.2.1.

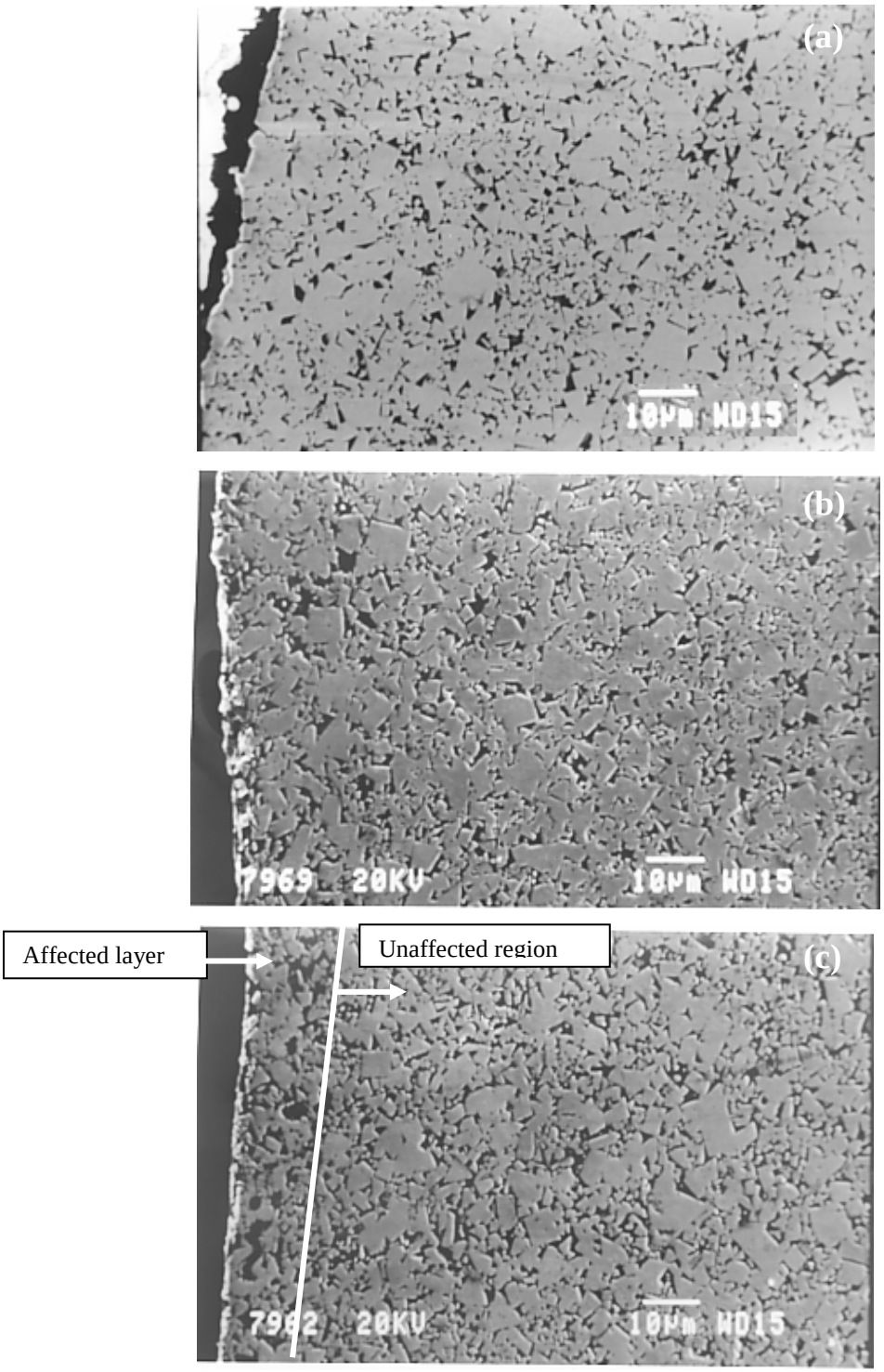


Figure 4.47: SEM micrographs of the cross-section of WC-12wt%Co at the edge. (a) is as received, (b) is after 60 cycles of thermal shock at 600°C and (c) is after 60 cycles of thermal shock at 800°C, showing possible affected layer near the edge.

EDS analysis of a sample after thermal shock was done on a polished cross-section to study if the affected layer in Figure 4.47C was due to cobalt depletion. However, the EDS spectra showed approximately the same Co peak intensity throughout the material, thus no cobalt depletion could be detected using the EDS. See Figures 4.49 to 4.52. This was also observed by other authors who found no visible cobalt depletion after rock drilling on samples affected by thermal shock using the EDS [2, 16].

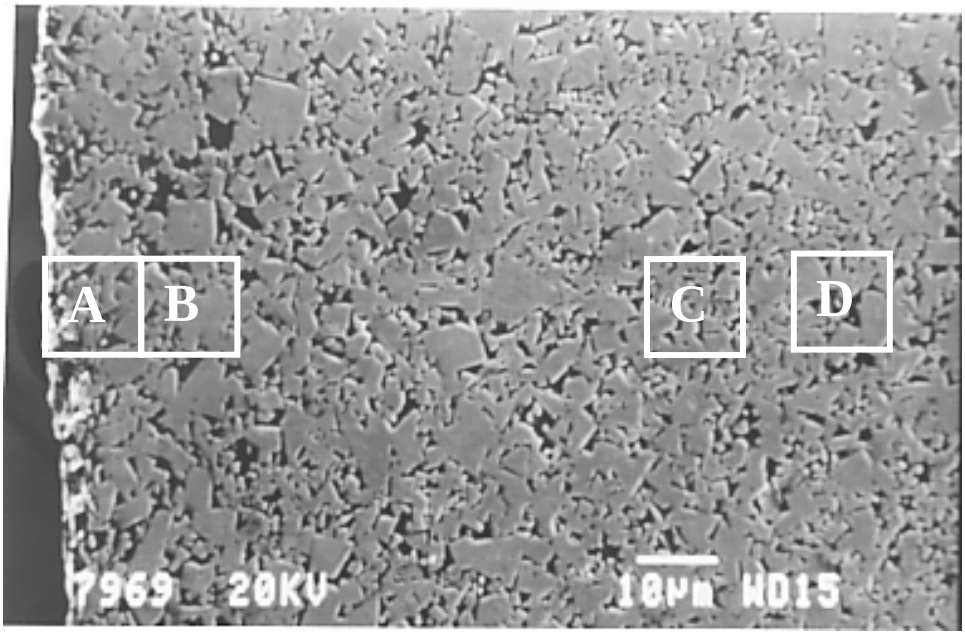


Figure 4.48: Same micrograph as in figure 4.47(c), showing square boxes where the area EDS spectra were taken.

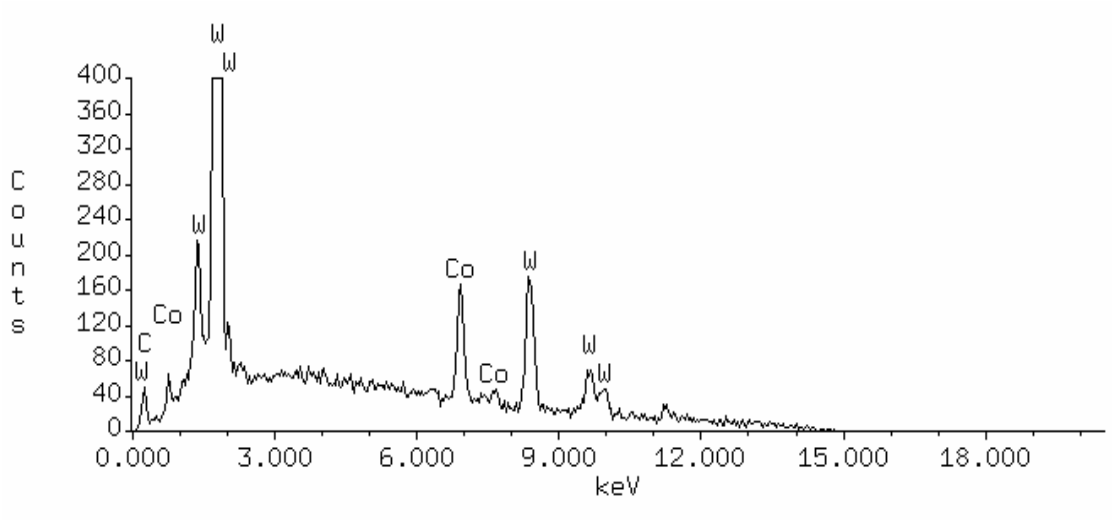


Figure 4.49: EDS spectrum of area A.

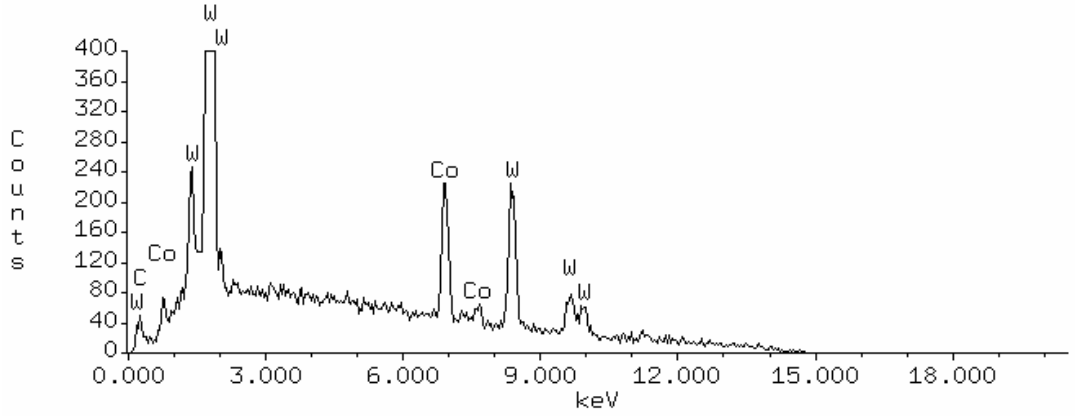


Figure 4.50: EDS spectrum of area B.

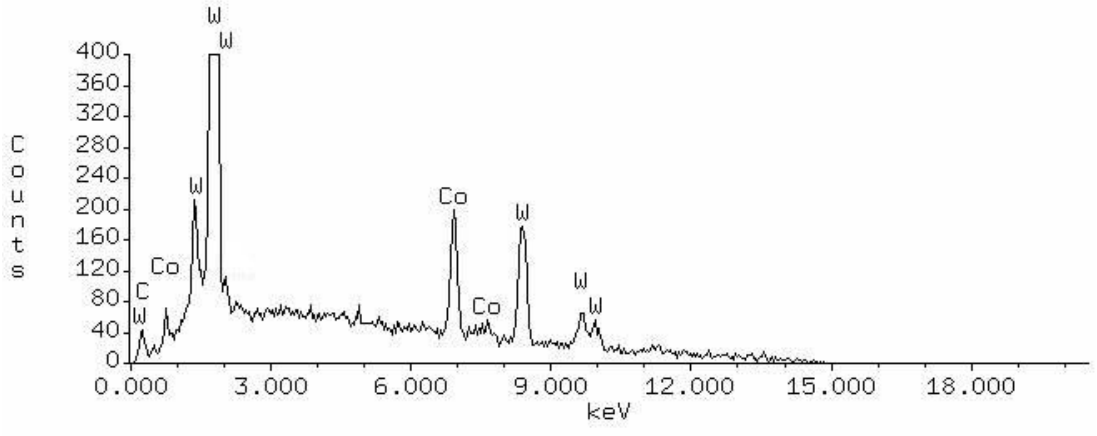


Figure 4.51: EDS spectrum of area C.

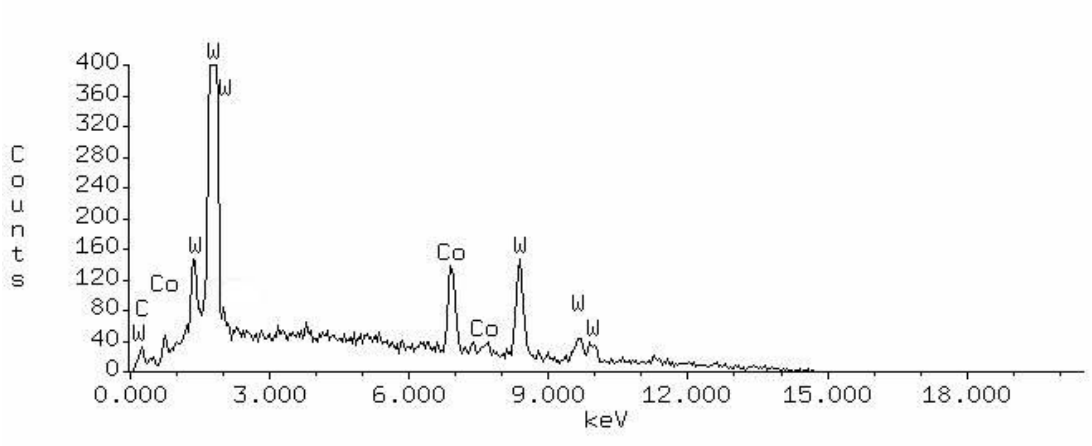


Figure 4.52: EDS spectrum of area D.

4.3.3.2 Damaged edges after thermal shock

Further analysis of the cross-sectioned samples after thermal shock was done to find any features that would affect the wear rate. In this project, SEM examination after thermal shock of the cross-sections revealed cracks parallel to the surface, cracked WC grains, that weakens the surface in higher degree than in samples without thermal shock. All the cracks observed appear to have formed in the subsurface layer 1 micron from the surface. See Figures 4.53 to 4.58 for these features.

It is known from previous investigations that a surface with a partially depleted binder phase weakens the surface, thus increasing the wear rate when the sample is exposed to wear [16]. This feature was found in all the tests done (60, 80, and 100 thermal shock cycles at 800°C, 60 thermal shock cycles at 600°C and 1000°C).

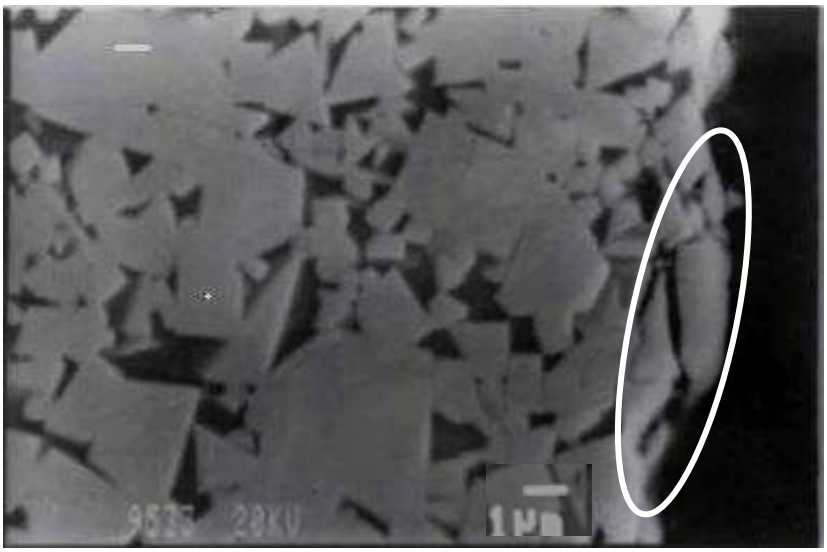


Figure 4.53: Crack in one grain of WC on the edge of sample after 100 cycles of thermal shock at 800°C which will promote more mechanical interlocking between the rough surface and the SiC abrasive paper thus increase the wear rate.

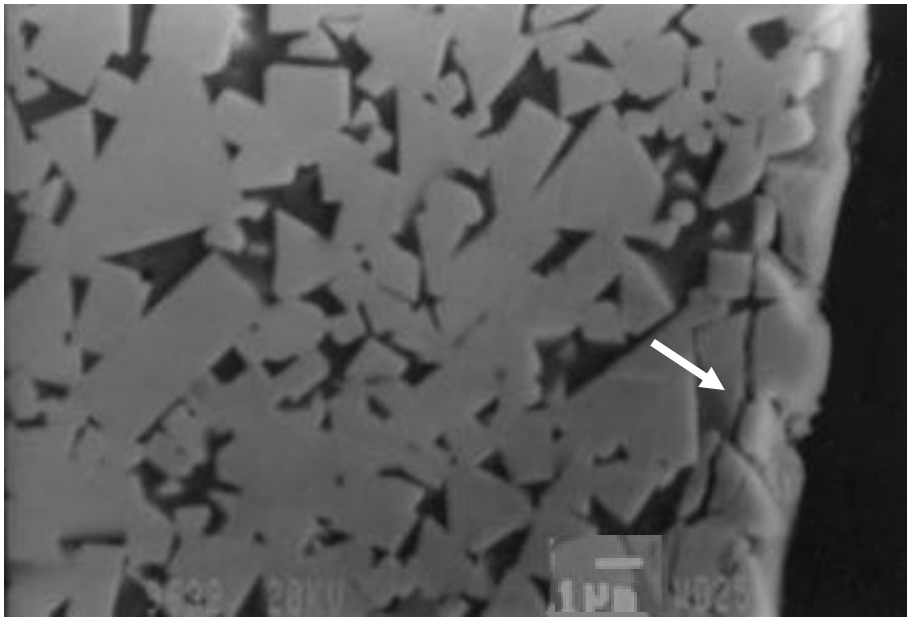


Figure 4.54: Crack along the edge of sample after 60 cycles of thermal shock at 1000°C which can lower the surface fracture strength and promote crack propagation during abrasive wear.

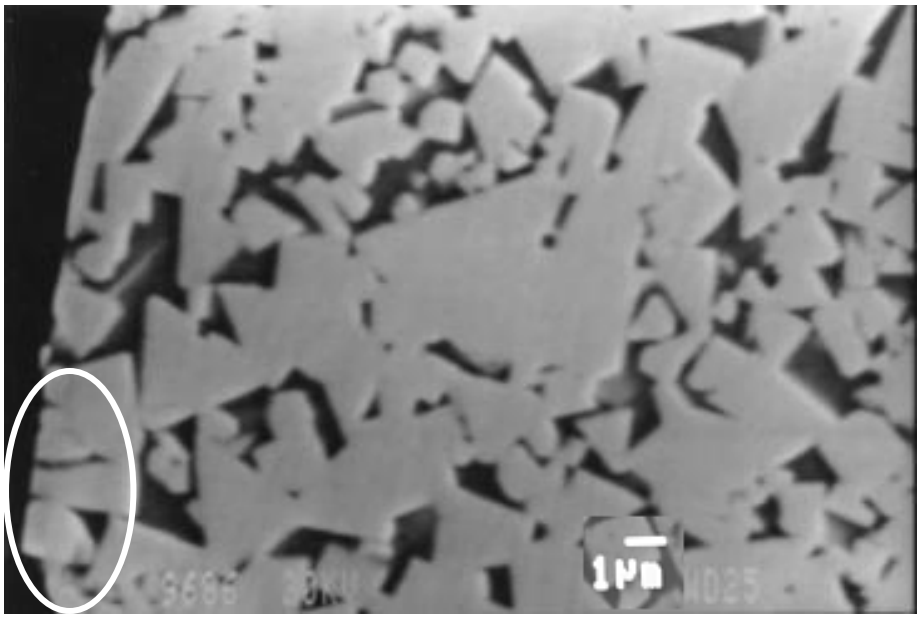


Figure 4.55: Cracked WC grain after 80 cycles of thermal shock at 800°C.

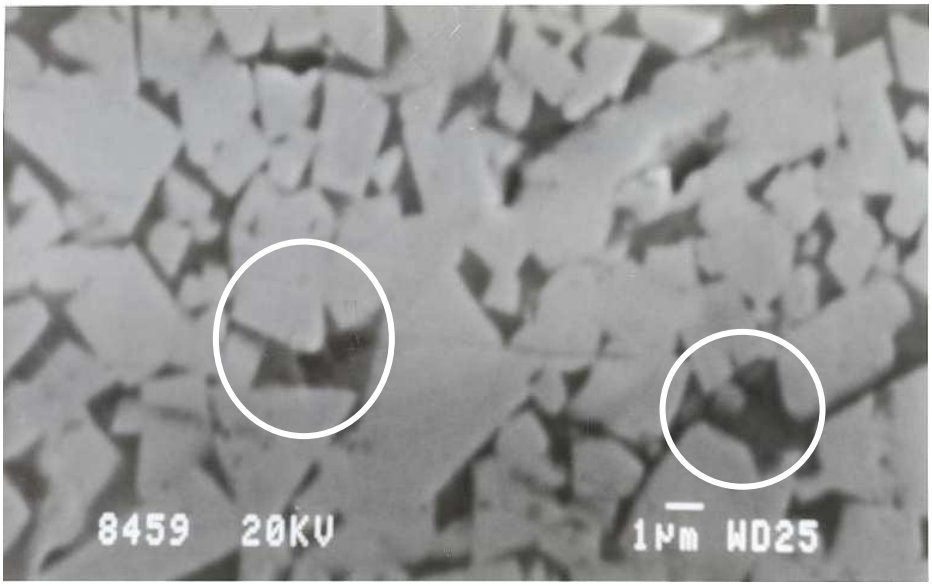


Figure 4.56: Voids between the WC grains after 60 cycles of thermal shock at 800°C, near the edge. This can also increase the wear rate by weakening the edge.

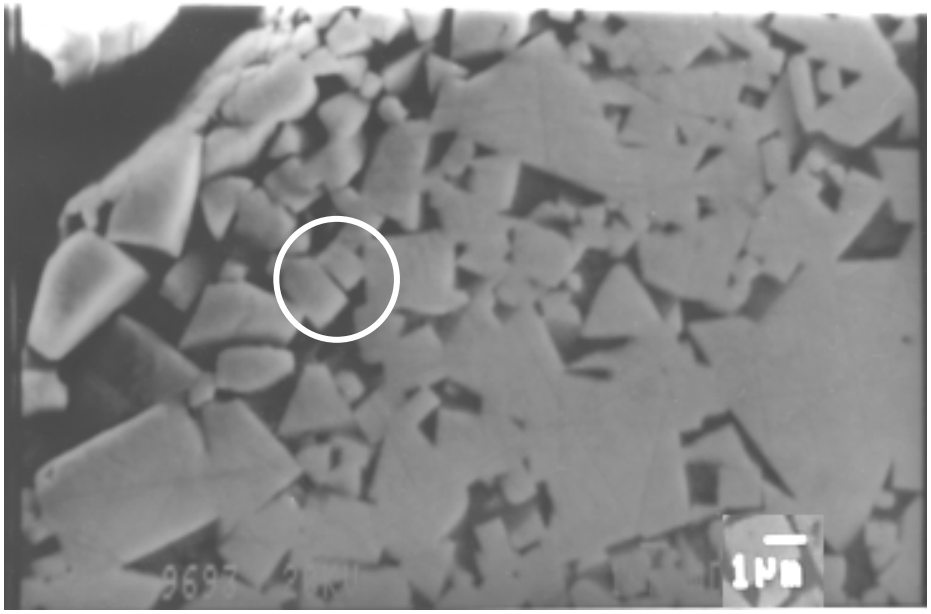


Figure 4.57: WC grains after 60 cycles of thermal shock at 1000°C showing possible cracked grains, which can be easily removed during wear.

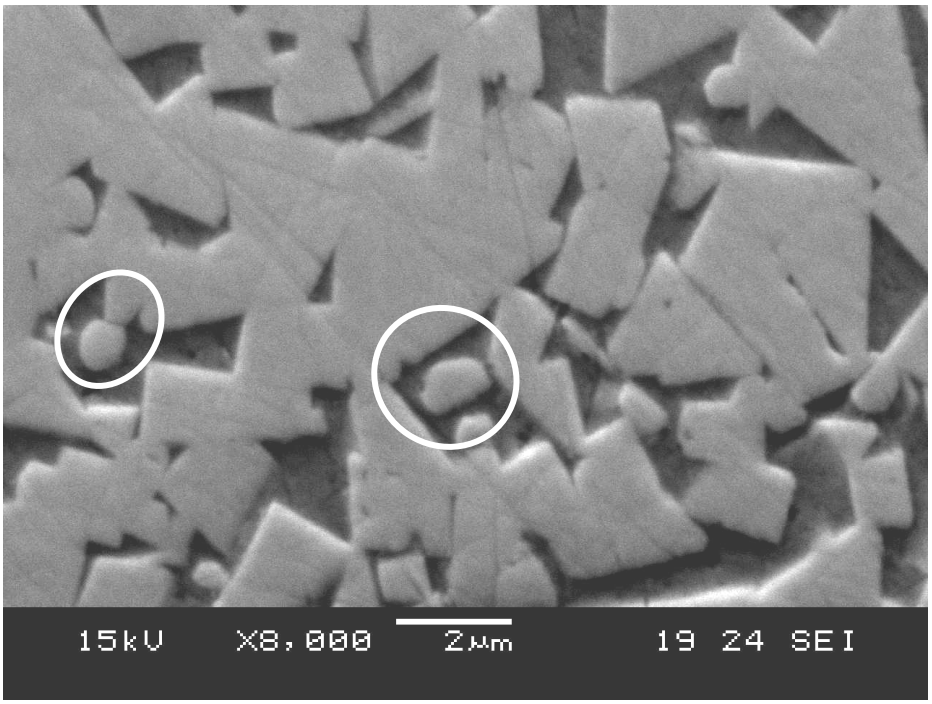


Figure 4.58: SEM micrograph of a cross-section after 60 cycles of thermal shock at 1000°C showing signs of round grains after thermal shock. This may decrease the hardness of the material by decreasing the contiguity in the WC-12wt%Co.

Rounded grains can be due to increased solubility of WC in Co at high temperature. The higher solubility affects the corners of the WC grains, which would dissolve first.

4.3.3.3 Microprobe analysis

The electron microprobe was used to establish the composition near the edge of cross-sectioned specimens (see Section 3.5.4 for more details about microprobe analysis). This was done to confirm the cobalt depletion observed during the SEM surface and cross-sectional analysis, since the EDS analysis of the cross-section had not shown cobalt depletion after thermal shock. In this investigation Tungsten, Cobalt, Carbon and Oxygen were the only elements scanned and the results were measured in weight percent then converted to atomic percent. Two scans were done on each sample as stated in section 3.5.4 (see Figure 4.59).

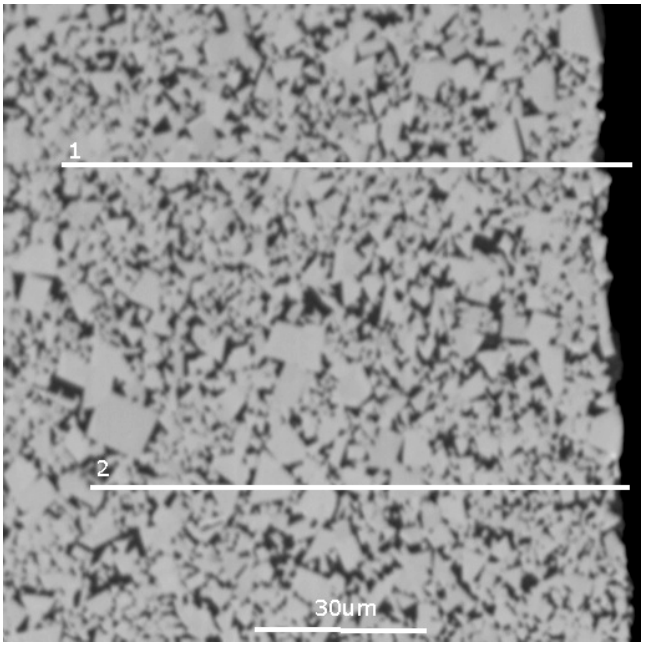


Figure 4.59: Micrograph of a cross-section showing two lines followed during the microprobe scans.

The scanning proceeded from 50 microns before the edge to the surface of the sample; therefore 0 micron in the graph represents the starting point. From figures 4.61 to 4.66, the W and C percent increase and decrease together because they are bonded in WC and this is clear in the atomic % patterns. Depletion of Co can possibly be observed by having low Co peaks near the edge and maybe higher on the edge due to migration. The O in the patterns must be due to surface oxidation, which was also observed, using EDS. Some of the line scans showed possible WC decarburization only at the edge after thermal shock, i.e. the W and the C patterns where observed to be parallel up to the edge but near the edge they stopped being parallel. Decarburization happens when oxygen reacts with C in WC and forms carbon monoxide, which is a gas and is lost; leaving WC poor of C. The decarburization reactions in this case will be:

Inferred

$$2WC + O \rightarrow CO + W_2C$$

The depth of depletion could not be determined, because it is random.

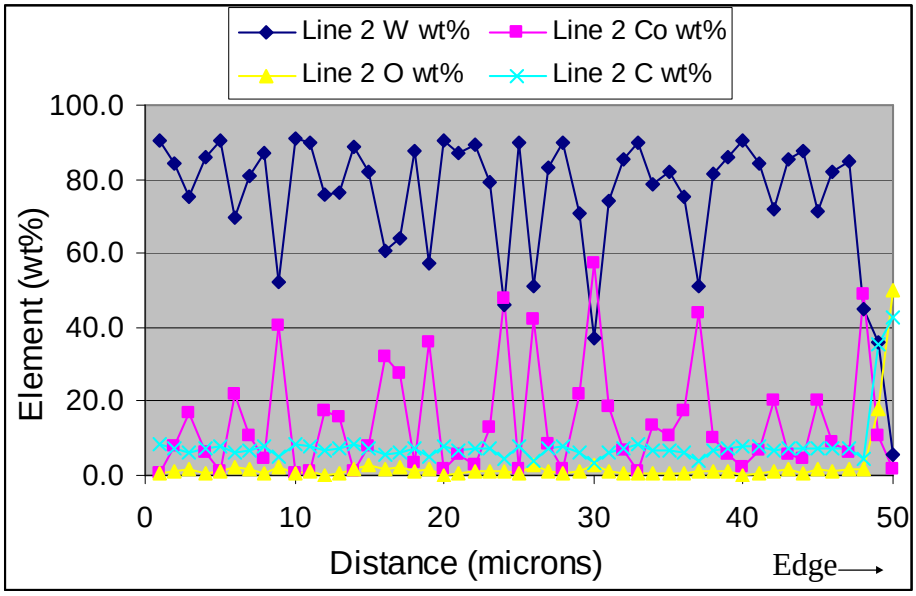
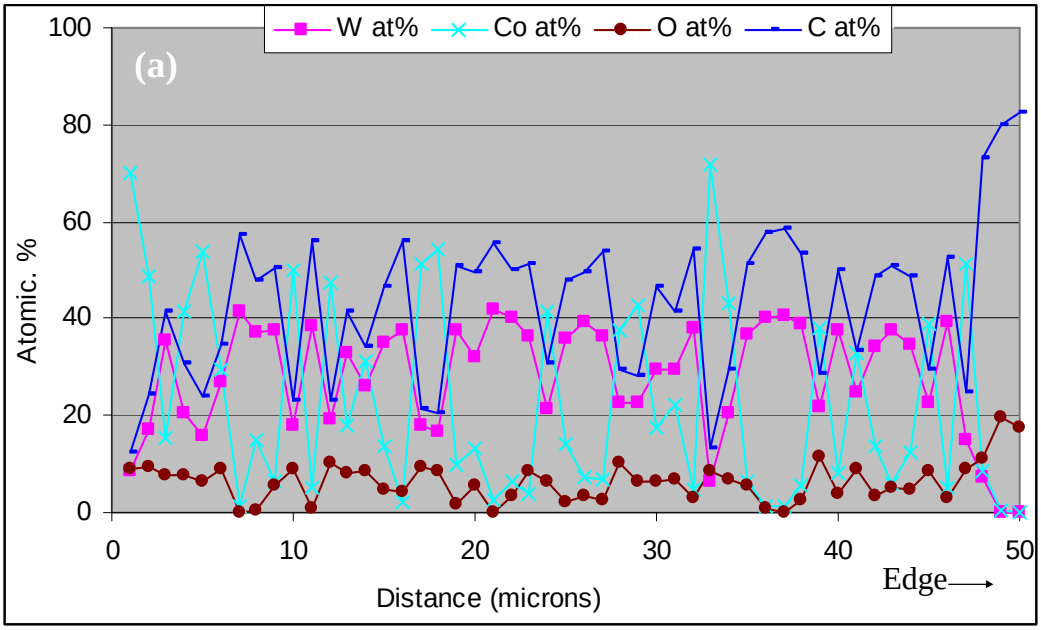


Figure 4.60: Line-scan of elements in weight percent from sample without thermal shock.



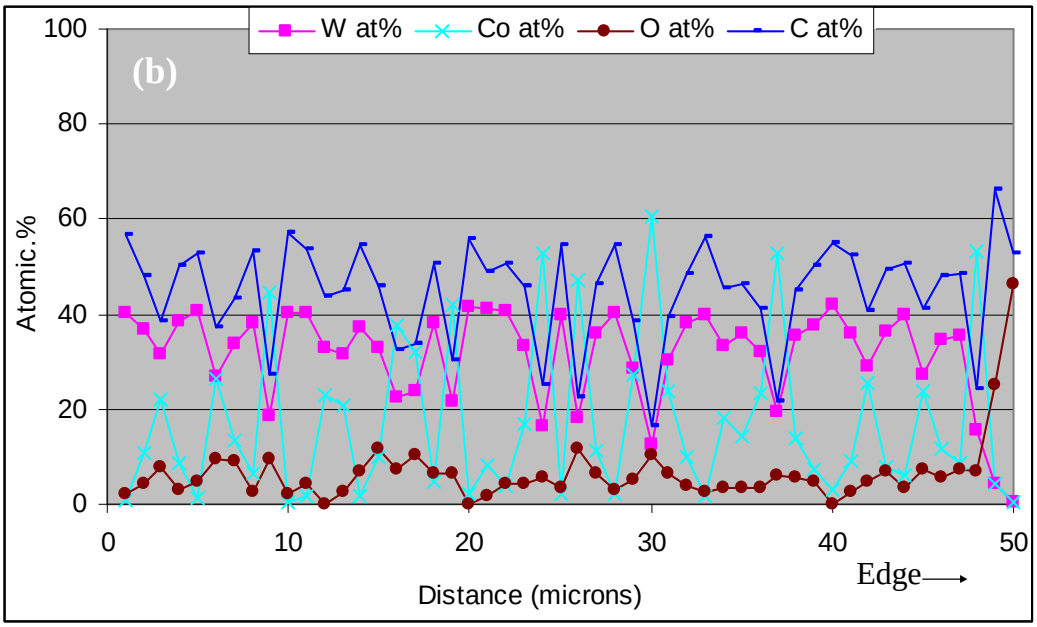


Figure 4.61: Line-scans of elements in atomic percent from sample without thermal shock. No cobalt depletion was observed at either (a) and (b). High carbon and oxygen at the edge was in the bakelite resin.

.

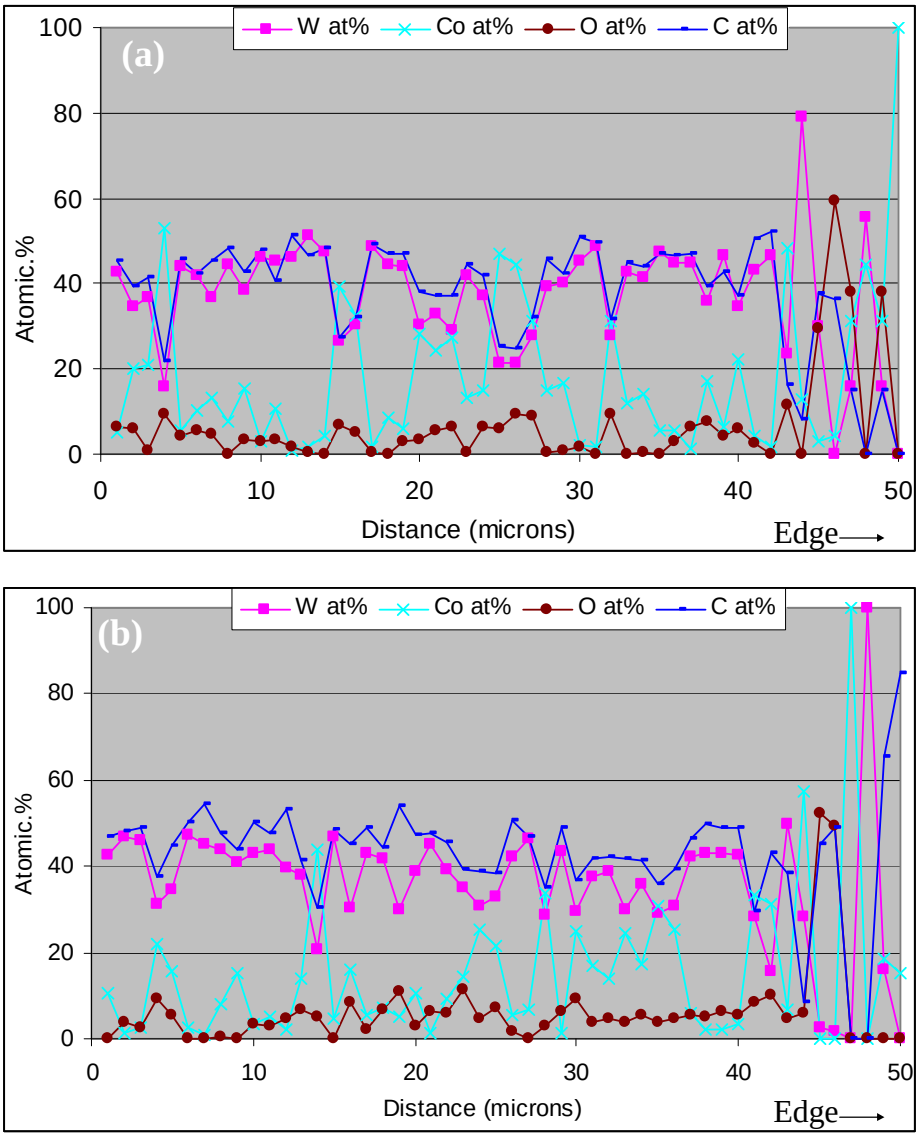


Figure 4.62: Line-scans in element atomic percent after 60 cycles of thermal shock at 600°C. On (a) the W and the C lines appear differently from about 5 microns from the edge. The high Co peak at the surface (50μm) may suggest Co migration to the surface and the oxygen peak increase near the edge suggests oxidation. No cobalt depletion was observed on (b), but some Co seems to have migrated to the surface. The possibility of decarburization of about 3 microns is observed near the edge because the W and C line scans have changed. The O at% peaks is higher from about 4 microns below the edge, which suggest oxide formation.

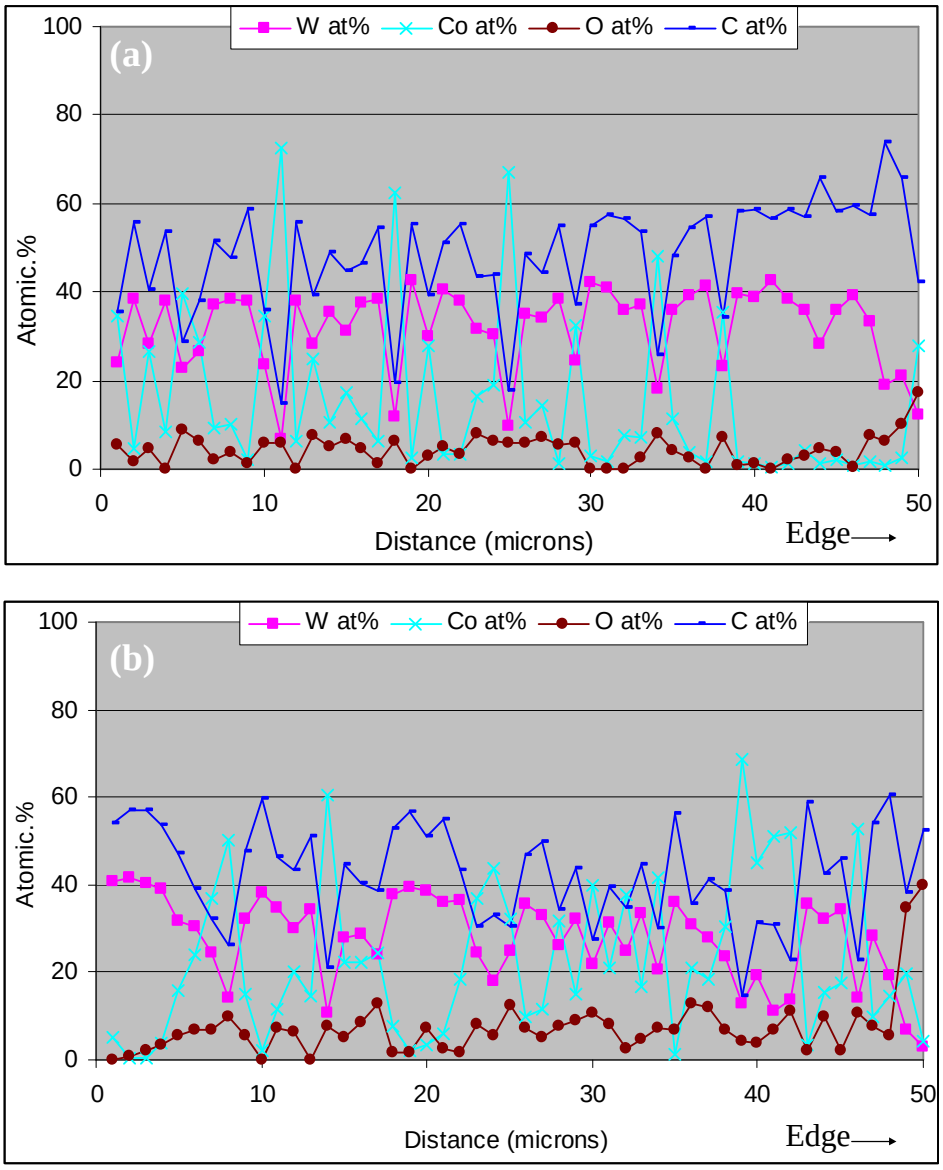


Figure 4.63: Line-scans in element atomic percent after 60 cycles of thermal shock at 800°C. No decarburization was observed in (a), the line scanned through a large WC grain of about 10µm near the edge. The at% of C is consistently higher than the at% of W. On (b) the W and the C lines are parallel until the start of the Bakelite(in which the sample was mounted i.e. no decarburization is observed.

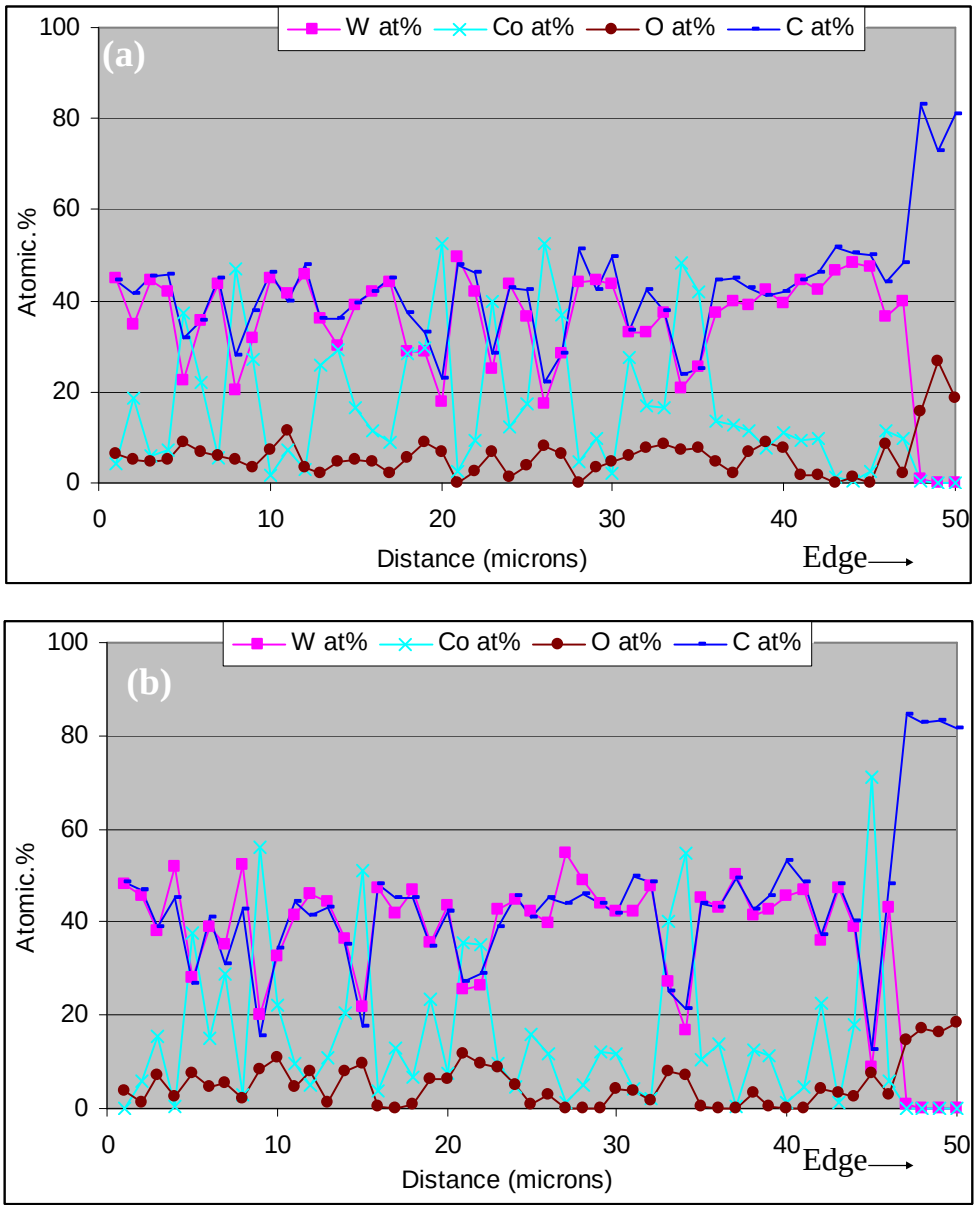


Figure 4.64: Line-scans in element atomic percent after 80 cycles of thermal shock at 800°C. Three points from the edge in (a) show high atomic percentages of oxygen and carbon implying that they were acquired from the bakelite. The composition of the bakelite is approximately 78% carbon, 18% oxygen and 5% hydrogen. From about 3 microns from the edge of both Figure 4.64(a) and (b) the scans where acquired on Bakelite. The W and the C patterns are parallel until the start of the Bakelite.

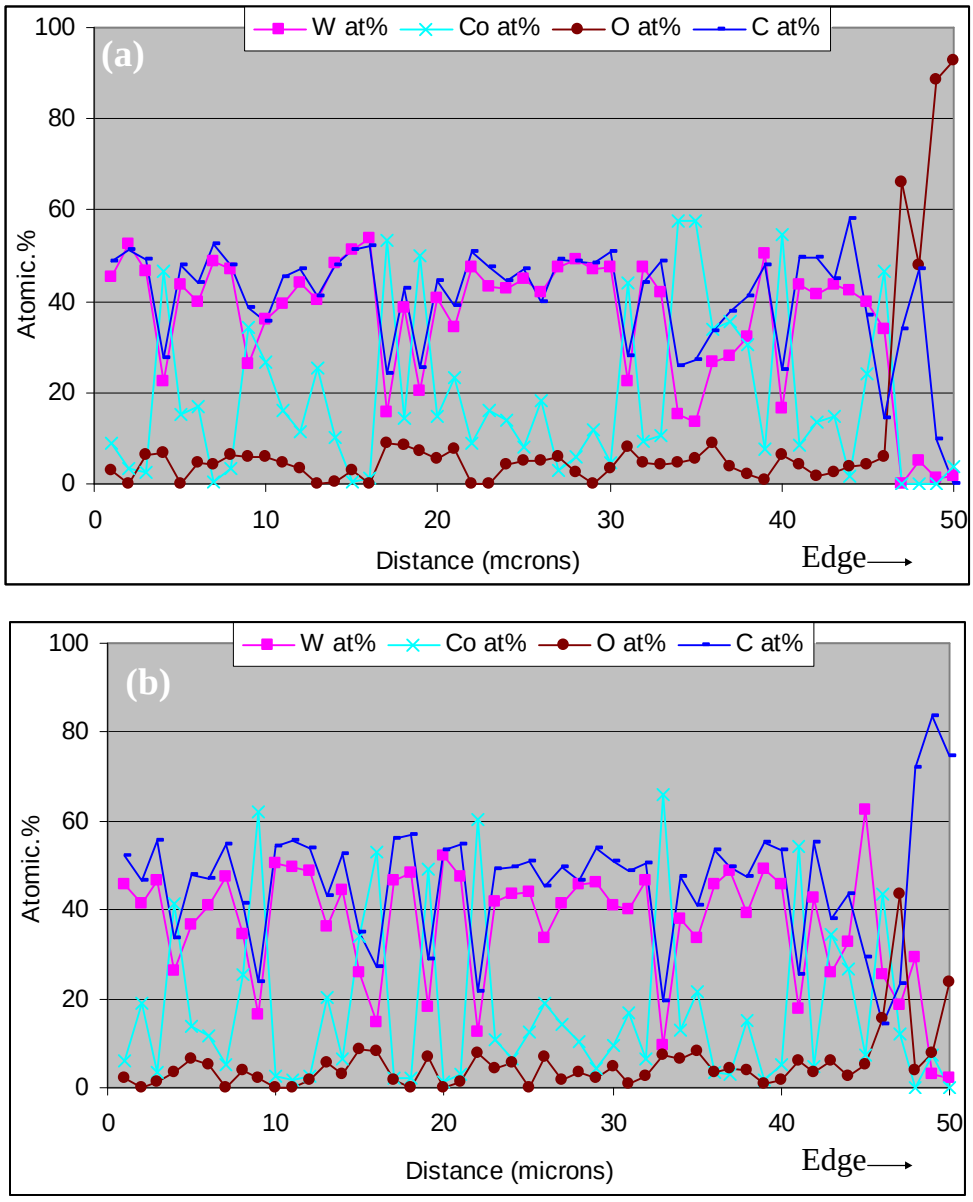


Figure 4.65: Line-scans in element atomic percent after 100 cycles of thermal shock at 800°C. From about 4 microns from the edge of figure 4.65 (a) Bakelite position because both the W and the Co are zero atomic %. No decarburization is observed. From about 6 microns from the edge of figure 4.65 (b) the W and C lines scans appear differently which may suggest decarburization of WC, i.e. formation of W_2C.

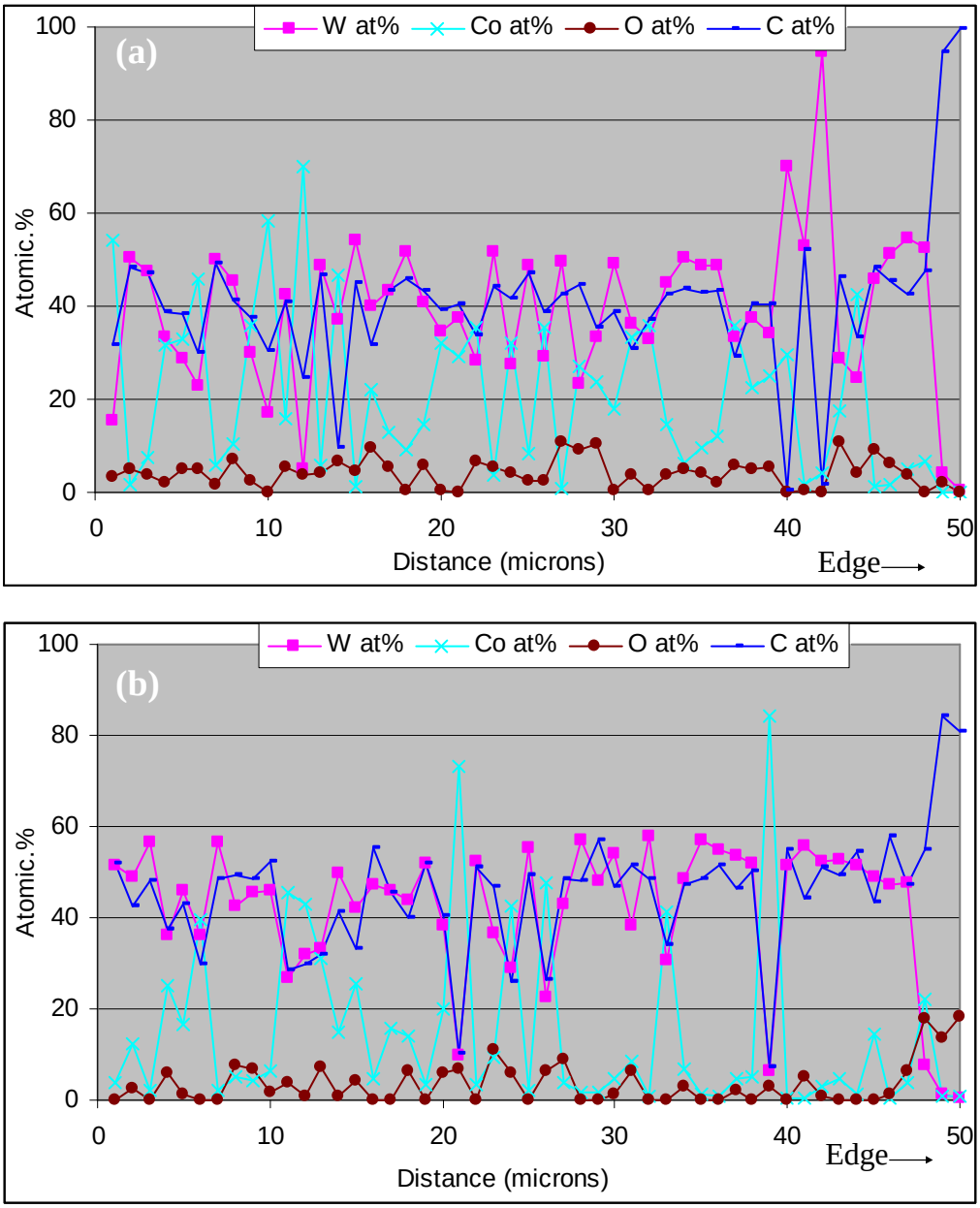


Figure 4.66: Line-scans in element atomic percent after 60 cycles of thermal shock at 1000°C. The W and the C lines in figure 4.66(a) appear differently at about 10 microns from the edge, which may indicate decarburization. No decarburization is observed at (b) i.e. the W and the C line scans appear the same until the start of the Bakelite, which is about 3 microns from the edge.

4.4 Effect of immersing WC-12wt%Co in water

WC-Co is known to exhibit corrosion pits when immersed in water [4]. Some authors associate pitting with contamination in the WC-Co, which acts as a driving force for corrosion. This investigation on the effect of water was done to explain observations after quenching WC-12wt%Co in water, where calcium-containing particles were observed. WC-12wt%Co was immersed in room temperature water for 12 hours. The surface was then observed using an SEM (see Figures 4.67 to 4.69).

The surface looked slightly etched; it is known that WC is corroded by alkalis (e.g. NaOH or KOH in Murakami's solution) and these may be present in water. White particles similar to those observed after thermal shock (Section 4.3.2.1) were observed after allowing the water to dry on the surface, which confirms that the white particles are related to salts that were in solution in the water and were left on the surface when the water evaporated.

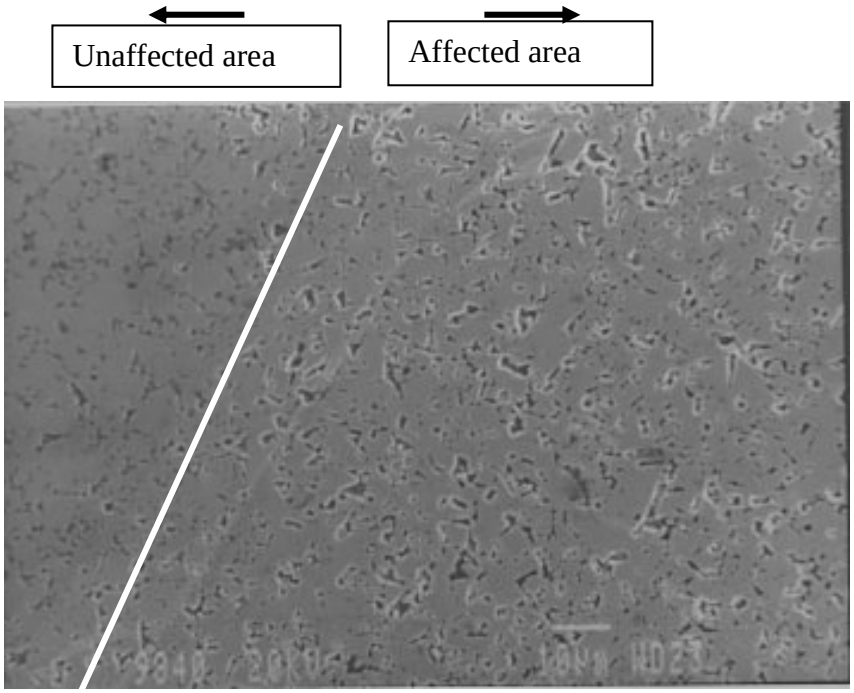


Figure 4.67: Surface appearance of WC-12wt%Co after being immersed in cold water for 12 hours, area to the right looks etched (affected area) while the other(to the left) is still unaffected by water. The etched areas were random after immersing in water.

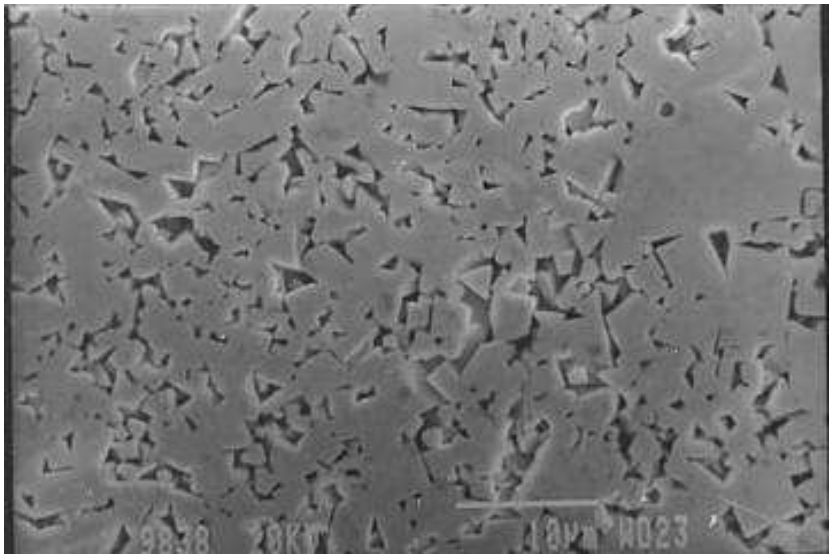


Figure 4.68: Closer view of the surface of WC-12wt%Co immersed in cold water. The surface looks etched.

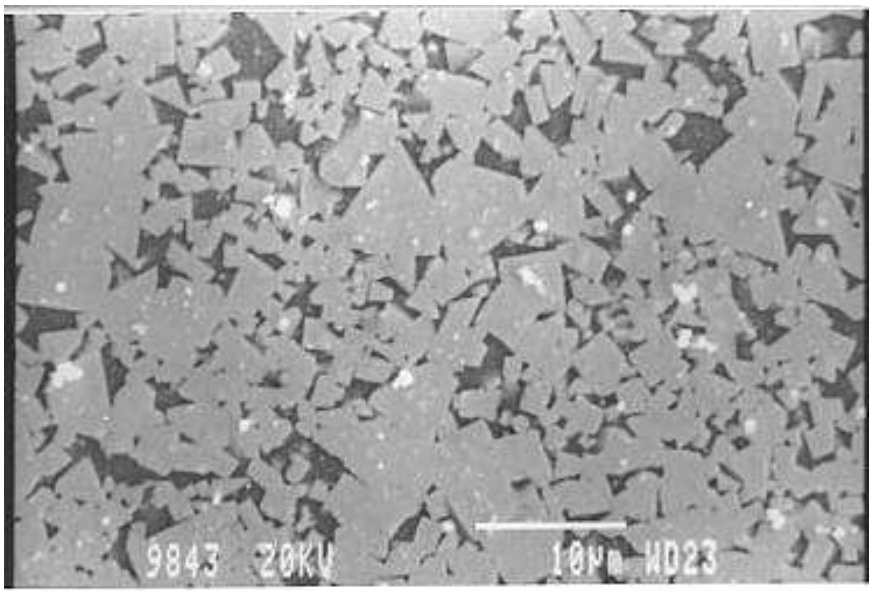


Figure 4.69: WC-12wt%Co alloy immersed in cold water. White particles are observed. This surface looks similar to those after 60 cycles of thermal shock at 600°C, 800°C and 1000°C.